



Univerza v Mariboru

Fakulteta za energetiko

Journal of ENERGY TECHNOLOGY



Volume 5 / Issue 3

AUGUST 2012

www.fe.uni-mb.si/si/jet.html

JOURNAL OF ENERGY TECHNOLOGY



VOLUME 5 / Issue 3

Revija Journal of Energy Technology (JET) je indeksirana v naslednjih bazah: INSPEC[®], Cambridge Scientific Abstracts: Abstracts in New Technologies and Engineering (CSA ANTE), ProQuest's Technology Research Database.

The Journal of Energy Technology (JET) is indexed and abstracted in the following databases: INSPEC[®], Cambridge Scientific Abstracts: Abstracts in New Technologies and Engineering (CSA ANTE), ProQuest's Technology Research Database.

JOURNAL OF ENERGY TECHNOLOGY

Ustanovitelji / FOUNDERS

Fakulteta za energetiko, UNIVERZA V MARIBORU /
FACULTY OF ENERGY TECHNOLOGY, UNIVERSITY OF MARIBOR

Izdajatelj / PUBLISHER

Fakulteta za energetiko, UNIVERZA V MARIBORU /
FACULTY OF ENERGY TECHNOLOGY, UNIVERSITY OF MARIBOR

Izdajateljski svet / PUBLISHING COUNCIL

Zasl. prof. dr. Dali ĐONLAGIĆ,

Univerza v Mariboru, Slovenija, **predsednik** / University of Maribor, Slovenia, **President**

Prof. dr. Bruno CVIKL,

Univerza v Mariboru, Slovenija / University of Maribor, Slovenia

Prof. ddr. Denis ĐONLAGIĆ,

Univerza v Mariboru, Slovenija / University of Maribor, Slovenia

Prof. dr. Danilo FERETIĆ,

Sveučilište u Zagrebu, Hrvatska / University in Zagreb, Croatia

Prof. dr. Roman KLASINC,

Technische Universität Graz, Avstrija / Graz University Of Technology, Austria

Prof. dr. Alfred LEIPERTZ,

Universität Erlangen, Nemčija / University of Erlangen, Germany

Prof. dr. Milan MARČIČ,

Univerza v Mariboru, Slovenija / University of Maribor, Slovenia

Prof. dr. Branimir MATIJAŠEVIČ,

Sveučilište u Zagrebu, Hrvatska / University in Zagreb, Croatia

Prof. dr. Borut MAVKO,

Inštitut Jožef Stefan, Slovenija / Jozef Stefan Institute, Slovenia

Prof. dr. Greg NATERER,

University of Ontario, Kanada / University of Ontario, Canada

Prof. dr. Enrico NOBILE,

Università degli Studi di Trieste, Italia / University of Trieste, Italy

Prof. dr. Iztok POTRČ,

Univerza v Mariboru, Slovenija / University of Maribor, Slovenia

Prof. dr. Andrej PREDIN,

Univerza v Mariboru, Slovenija / University of Maribor, Slovenia

Prof. dr. Jože VORŠIČ,

Univerza v Mariboru, Slovenija / University of Maribor, Slovenia

Prof. dr. Koichi WATANABE,

KEIO University, Japonska / KEIO University, Japan

Odgovorni urednik / EDITOR-IN-CHIEF

Andrej PREDIN

Uredniki / CO-EDITORS

Jurij AVSEC

Miralem HADŽISELIMOVIĆ
Gorazd HREN
Milan MARČIČ
Jože PIHLER
Iztok POTRČ
Janez USENIK
Peter VIRTič
Jože VORŠIČ

Uredniški odbor / EDITORIAL BOARD

Prof. dr. Jurij AVSEC,

Univerza v Mariboru, Slovenija / University of Maribor, Slovenia

Prof. ddr. Denis ĐONLAGIĆ,

Univerza v Mariboru, Slovenija / University of Maribor, Slovenia

Doc. dr. Željko HEDERIĆ,

Sveučilište Josipa Jurja Strossmayera u Osijeku, Hrvatska / Josip Juraj Strossmayer University
Osijek, Croatia

Doc. dr. Miralem HADŽISELIMOVIĆ,

Univerza v Mariboru, Slovenija / University of Maribor, Slovenia

Doc. dr. Gorazd HREN,

Univerza v Mariboru, Slovenija / University of Maribor, Slovenia

Prof. dr. Roman KLASINC,

Technische Universität Graz, Avstrija / Graz University Of Technology, Austria

dr. Ivan Aleksander KODELI,

Institut Jožef Stefan, Slovenija / Jožef Stefan Institute, Slovenia

Prof. dr. Jurij KROPE,

Univerza v Mariboru, Slovenija / University of Maribor, Slovenia

Prof. dr. Alfred LEIPERTZ,

Universität Erlangen, Nemčija / University of Erlangen, Germany

Prof. dr. Branimir MATIJAŠEVIĆ,

Sveučilište u Zagrebu, Hrvaška / University of Zagreb, Croatia

Prof. dr. Matej MENCINGER,

Univerza v Mariboru, Slovenija / University of Maribor, Slovenia

Prof. dr. Greg NATERER,

University of Ontario, Kanada / University of Ontario, Canada

Prof. dr. Enrico NOBILE,

Università degli Studi di Trieste, Italia / University of Trieste, Italy

Prof. dr. Iztok POTRČ,

Univerza v Mariboru, Slovenija / University of Maribor, Slovenia

Prof. dr. Andrej PREDIN,

Univerza v Mariboru, Slovenija / University of Maribor, Slovenia

Prof. dr. Aleksandar SALJNIKOV,

Univerza Beograd, Srbija / University of Beograd, Serbia

Prof. dr. Brane ŠIROK,

Univerza v Ljubljani, Slovenija / University of Ljubljana, Slovenia

Doc. dr. Andrej TRKOV,

Institut Jožef Stefan, Slovenija / Jožef Stefan Institute, Slovenia

Prof. ddr. Janez USENIK,

Univerza v Mariboru, Slovenija / University of Maribor, Slovenia

Doc. dr. Peter VIRTIČ,

Univerza v Mariboru, Slovenija / University of Maribor, Slovenia

Prof. dr. Jože VORŠIČ,

Univerza v Mariboru, Slovenija / University of Maribor, Slovenia

Prof. dr. Koichi WATANABE,

KEIO University, Japonska / KEIO University, Japan

Prof. dr. Mykhailo ZAGIRNYAK,

Kremenchuk Mykhailo Ostrohradskyyi National University, Ukrajina / Kremenchuk Mykhailo Ostrohradskyyi National University, Ukraine,

Doc. dr. Tomaž ŽAGAR,

Univerza v Mariboru, Slovenija / University of Maribor, Slovenia

Doc. dr. Franc ŽERDIN,

Univerza v Mariboru, Slovenija / University of Maribor, Slovenia

Tehniška podpora / TECHNICAL SUPPORT

Tamara BREČKO BOGOVČIČ,

Sonja NOVAK,

Janko OMERZU;

Izhajanje revije / PUBLISHING

Revija izhaja štirikrat letno v nakladi 150 izvodov. Članki so dostopni na spletni strani revije - www.fe.uni-mb.si/si/jet.html / The journal is published four times a year. Articles are available at the journal's home page - www.fe.uni-mb.si/si/jet.html.

Cena posameznega izvoda revije (brez DDV) / price per issue (VAT not included in price):
50,00 EUR

Informacije o naročninah / subscription information:

<http://www.fe.uni-mb.si/si/narocnine/index.php>

Lektoriranje / LANGUAGE EDITING

Terry T. JACKSON

Oblikovanje in tisk / DESIGN AND PRINT

Vizualne komunikacije comTEC d.o.o.

Oblikovanje revije in znaka revije / JOURNAL AND LOGO DESIGN

Andrej PREDIN

Revija JET je sofinancirana s strani Javne agencije za knjigo Republike Slovenije / The Journal of Energy Technology is co-financed by the Slovenian Book Agency.

Suša v Sloveniji, 2012

Letošnja suša se odraža tako na energetskem, okoljskem kot na prehrabnem področju. Narave ne moremo upravljati, čutimo pa posledice njene muhavosti. Najverjetneje smo z industrijskimi izpusti emisij in toplogrednih plinov sami zelo pripomogli k zdajšnjemu ekstremnemu vremenu, ki skokovito niha iz vročine v hlad, iz suše v neurja,

Tako nizkega vodostaja slovenskih rek že dolgo nismo zaznali. To se seveda direktno odraža na nižji proizvodnji električne energije v Sloveniji, ki meji že skorajda na katastrofo s hidroenergetskega stališča. Zato smo primorani uvažati električno energijo, saj je izpad proizvodnje hidroelektrarn tako velik, da ga s termo in jedrsko elektrarno ni možno pokriti. Navkljub nizkemu vodostaju slovenskih rek, imamo še neizkoriščen hidroenergetski vir, reko Muro – naš slovenski del. Avstrijski del oz. gornji tok reke Mure je že vrsto let praktično energetsko popolnoma izkoriščen. Postavljenih je že trideset hidroelektrarn.

Zanimivi so rezultati zadnjih meritev pretokov, ki kažejo, da so bili pretoki reke Mure v marčevskih dneh celo bolj ugodni od pretoka reke Drave, ki je naša energetsko najbolj izkoriščena reka. Žal je padec v spodnjem toku reke Mure precej manjši od padca reke Drave. Zato iz energetskega stališča, navkljub enakim pretokom, reki nista popolnoma primerljivi. V mesecu marcu letošnjega leta so znašali pretoki reke Mure 180 m³/s, reke Drave pa le 150 m³/s. Ta podatek ni pomemben le z vidika neizkoriščenega energetskega hidro potenciala reke Mure, ampak tudi dejstva, da se v Sloveniji, ob pričujoči suši, že danes srečujemo s pomanjkanjem vode tako v zadrževalnikih vode, kot tudi podtalnih voda. Po napovedih klimatologov bo pomanjkanje vode v prihodnosti še izrazitejše. Nedavno so geofiziki odkrili ozonsko »luknjo« tudi nad severnim tečajem, nad Arktiko, ki se je pojavila med lansko mrzlo zimo. Z meritvami so ugotovili, da se je razgradilo približno 40% ozona. Problem je še večji zato, ker je »Arktična ozonska luknja« zelo gibljiva, kar pomeni, da lahko seže tudi nad Evropo. Tudi zato je toliko bolj pomembno, da površinske - rečne vode čimdlje zadržimo na naših tleh. S tem ukrepom »damo vodi« več časa za njeno pronicanje v podtalne vode. To vlogo lahko med drugim prevzamejo tudi večnamensko grajeni akumulacijski bazeni hidroelektrarn, ki bi ob smiselni uporabi lahko služili tudi za namakanje polj oz. kot bistveni del namakalnih sistemov. Še posebej v Prekmurju, kot naši žitnici, bi takšni namakalni sistemi ob takšnih sušnih obdobjih prišli še kako prav. Zavedati se moramo dejstva, da v Sloveniji premalo pozornosti posvečamo skrbi za našo narodno prehrabno samooskrbo. Vse preveč smo že odvisni od tujine, ne samo na energetskem, tudi na prehrabnem področju. Z usklajeno energetsko, okoljsko in prehrabno politiko, bi lahko storili več za dobrobit Slovenije. Na teh področjih bi lahko iskali izhod iz sedanje krize.

Krško, avgust 2012

Andrej PREDIN

Drought in Slovenia, 2012

This year's drought is reflected in the energy and environmental fields, specifically affecting areas such as food production. Nature cannot manage; we feel the consequences of her whims. Most likely, we ourselves have helped to cause the current very extreme weather, which fluctuates dramatically from hot to cold, drought to flood, with our industrial discharges and emissions of greenhouse gases.

Such low water levels in Slovenian rivers have not been seen for a very long time. This is, of course, directly reflected in lower electricity production in Slovenia. The effects could almost be called disastrous for hydroelectric power production. We are forced to import electricity because the loss of hydropower production is so great that local thermal and nuclear power sources cannot compensate for it. Despite the low water levels of Slovenian rivers, we still have an unused source of hydroelectric power: the Slovenian part of the Mura River. The upper part of this river in Austria is practically fully exploited: thirty hydropower plants have already been built on it.

Interesting results of recent measurements of flow show that the capacity of the Mura River in March is even more favourable than the flow of the Drava River, which is our most energy-utilised river. Unfortunately, the head of the Mura is much smaller than the head of the Drava. Therefore, from the energy point of view, the rivers are not fully comparable. In March of this year, the capacity of the Mura was 180 m³/s, and the Drava's was only 150 m³/s. This information is important not only in terms of the unused hydro-energy potential of the Mura River, but also in the fact that in the present drought Slovenia is faced with the problems of water shortages in surface reservoirs as well as groundwater storage. According to the forecasts of climatologists, water shortages will be even more pronounced in the future. Recently, geophysics discovered an ozone 'hole' over the North Pole, above the Arctic, which occurred during last year's cold winter; almost 40% of the ozone was gone. The problem is even greater because the 'Arctic ozone hole' is very flexible, which means that it can reach Europe. This means that the influence of ozone hole could be expected also in our areas.

This year's drought is a warning that we must retain the surface water on our soil as much as possible. This measure leads to the fact that the surface water has more time to flow into the groundwater. This could be achieved with the construction of multipurpose hydroelectric dams that can also serve for the irrigation of fields. Especially in Prekmurje, the north-eastern part of Slovenia, such irrigation systems could be very useful during such dry periods. Slovenia is still not sufficiently aware of the importance of food self-sufficiency. We are already too dependent, both for energy but also for food, on foreign sources. Coordinating energy, environmental and food policy could do more for the welfare of Slovenia, and provide a way out from the current crisis.

Table of Contents /

Kazalo

Method of rational choice of some electromechanical devices and their series / Metoda racionalne izbire nekaterih elektromehanskih naprav <i>M. V. Zagirnyak, V. V. Prus, A. V. Nikitina</i>	11
A fuzzy model of power supply system control / Mehki model upravljanja energetskega sistema <i>Janez Usenik</i>	23
Fracture toughness of heterogeneous energy components / Lomna žilavost heterogenih energetskega komponent <i>Zdravko Praunseis</i>	39
Isentropic efficiency of gas turbine axial compressors and the outdoor temperature effect / Izentropski izkoristek aksialnega turbokompresorja plinske turbine in vpliv zunanje temperature <i>Josip Gašparinčič, Aleš Štriclej</i>	47
Rain energy as a green energy source? / Dež kot zeleni energetski vir? <i>Andrej Predin, Gorazd Hren</i>	59
Mathematical models for the simulation of pumps systems / Matematični modeli za simulacijo črpalnih sistemov <i>Mitja Kastrevc, Edvard Detiček</i>	65
Instructions for authors	77

METHOD OF RATIONAL CHOICE OF SOME ELECTROMECHANICAL DEVICES AND THEIR SERIES

METODA RACIONALNE IZBIRE NEKATERIH ELEKTROMECHANSKIH NAPRAV

M.V. Zagirnyak[✉], V.V. Prus, A.V. Nikitina

Keywords: electric machine, transformer, electric device, generalised linear dimension.

Abstract

An approach to improvement of interconnections of a summarised geometric dimension and the power parameters of electric machines, transformers and electric devices is determined based on a generalisation of theoretical and experimental research results.

Povzetek

Delo obravnava pristop iskanja povezav med elektromagnetnimi parametri in geometrijo različnih vrst električnih strojev ter ostalih električnih naprav. Na podlagi rezultatov teoretičnih in eksperimentalnih raziskav je oblikovan kriterij, ki omogoča racionalno izbiro družine električnih naprav za izbrane moči.

[✉] Corresponding author: Mykhaylo Zagirnyak, D.Sc. (Eng.), Prof., Tel.: +38 05366 36218, Fax: +38 05366 36000, Mailing address: Kremenchuk Mykhailo Ostrohradskyi National University Vul. Pershotravneva, 20, 39600, Kremenchuk, Ukraine, E-mail address: mzagirn@kdu.edu.ua

1 INTRODUCTION

The existing trend to globalisation significantly broadens the possibilities of choosing electric machines (EM), transformers and electric devices (ED). Taking into consideration the diversity of their design and manufacturing technologies, as well as differences in the required properties of the materials used, it is necessary to develop assessment criteria enabling one to rationally choose particular devices or their series with similar operating characteristics. The choice is to be made taking into account comparisons of the efficiency of each device and the series in which they are manufactured. As a rule, the direct determination of efficiency is impossible due to the absence of detailed data concerning actual losses and electromagnetic loads. It can be explained as a result of insufficient information about a manufactured product in its producers' catalogues, which complicates the accurate direct comparison of particular devices, taking into account the impossibility of buying all available devices of different series to make an experimental comparison.

2 ANALYSIS OF THE PREVIOUS RESEARCH

Many research papers have been devoted to the problems of finding connection between the overall electromagnetic and power characteristics of EM, transformers, ED and their rational selection. However, to date, this problem has not been completely solved.

The assessment of separate devices and their series is to be based not only on comparison of the power characteristics used to choose the required device (such as power, windings voltage, short circuit and no-load loss, etc., influencing operating costs). It also should take into consideration mass overall parameters significantly influencing both the possibility of introducing devices into industrial equipment and cost parameters, [1].

Therefore, the specification of regularities connecting power and geometric dimensions of EM, transformers and ED is one way to create criteria for selecting them rationally.

At present, a series of dependences of the form

$$X = k\ell^n, \quad (2.1)$$

is considered to be generally accepted. It connects generalised linear dimension (GLD) ℓ with one of EM main parameters X , which can be presented by electromagnetic power S_{em} , armature current I_a , material consumption, mass M , volume V , etc. In (2.1) k is proportionality coefficient; n is exponent and an integral number as a rule.

The said relations are used for geometrically similar machines [2, 3].

It should be noted that in spite of the apparent simplicity, the relations of the form (2.1) are quite reliable and indirectly connected with such parameters as magnetic induction B and current density J , which, in turn are determined by the properties of magnetic and conducting materials, respectively, equal and geometrically similar EM, as well as the number of phases m .

The external diameter D_c of the EM magnet frame is usually considered to be a generalised linear dimension, as it is initially assumed to be most functionally connected with power.

In accordance with previous conceptions, EM material consumption, mass M and volume V

are proportional to the third power of GLD [1]. Total losses power $\sum \Delta P_i$ is also proportional to the third power of GLD. Cooling surface area S_c and total area of slots in geometrically similar EM are considered to be proportional to the second power of GLD, which results in the proportionality of linear current load A_o to GLD and the fourth power of S_{em} dependence on ℓ .

Analogous results for S_{em} can be obtained from formulas for machine constants of Arnold, Esson, Vidmar, Richter, Shenfer, Rushmel, [1, 3].

The results of the calculation show that the exponent in dependence (2.1) may differ greatly from the above-given values. It cannot be explained by the technology of EM production or change of design within the same series.

Such a discrepancy makes the problem of expanding the boundaries of known dependences of type (2.1) topical, as in their present form they cannot be directly used for the comparative assessment of EM belonging to different series because of the vagueness of values k and n .

There is practically no similar approach concerning transformers in the literature, which is connected with both the difficulties of GLD choice, especially for power transformers with oil tanks, and a general absence of research of this problem.

Regarding ED, this problem is more complicated because of the considerable diversity of their types and the necessity of determining significant parameters for each of them, as the value of electromagnetic power S_{em} is not determinative for them. Existing partial dependences connecting separate parameters of some ED types are not of a generalising character and are empirical.

3 PURPOSE OF THE PAPER

This paper has been written to provide a generalisation of functional interconnections of power and electromagnetic parameters of EM, transformers and ED with their geometric dimensions on the basis of the obtained dependences with the purpose of formation of criteria for their rational choice and determination of their improvement ways.

4 MATERIAL AND RESULTS OF THE RESEARCH

The choice of generalised linear dimension for EM, transformers and ED was substantiated in the process of research, [4–6].

Choice of GLD for EM. Rotation axis height h is to be considered GLD ℓ for EM as it shows minimal change of power dependence of EM parameters on GLD when examining one model after another in a series of industrial electric motors, [4].

Choice of GLD for transformers. Geometric mean of three overall dimensions (length L , breadth B and height H) was assumed to be GLD for transformers

$$\ell = \sqrt[3]{LBH} ;$$

$$\ell_b = \sqrt[3]{L_b B_b H_b} ,$$

where ℓ , ℓ_b is the GDL of series calculated transformer and the transformer assumed to be the basic one in the series, respectively; L_b, B_b, H_b are the corresponding dimensions of the basic transformer, [5].

Choice of GLD for ED. Geometric mean of three overall dimensions (length L , breadth B and height H) was assumed to be GLD for ED as for transformers, which made it possible to obtain stable relations connecting GLD with the pressure on the contacts, current density in windings and contacts, electric magnet tractive effort, etc., [6].

Calculated relations for EM, transformers and ED were substantiated during the research. They made it possible to connect GLD with their main operating parameters and to obtain a number of recommendations as to the peculiarities of their application in the choice of separate devices and their series.

Electric machines. The research results obtained for EM enabled the substantiation of the physical sense of using such parameters as current density, magnetic induction, frequency, shaft power and loss power when relations for their interconnection with GLD are obtained.

It has been proved that real values of index n considerably differ from the known values, [4], though the principle of geometric similarity of EM belonging to the same series usually holds. The difference of real indices from generally accepted is from -38% to +124%.

The obtained relations are different for different EM power ranges. Therefore, for low power EM and micromachines, the following dependence is true:

$$S_{em} = k_a k_{bB} \ell^5, \quad (4.1)$$

where k_a, k_{bB} are coefficients characterising the connection of EM electric and magnetic parameters, respectively, with GLD.

It should be noted that dependence character is influenced by EM excitation mode and frequency, which sometimes results in the decrease of the exponent to 1.5.

Regarding medium-power EM, except for special purpose machines, the conditions of constant influencing parameters are met as a rule, then equation (2.1) is true for them and electromagnetic power is a GLD function in the power range from 3.5 to 4, though the exponent may approach five at the beginning of the range.

In high power EM, current density can be considered constant, but the fact of centrifugal force influence cannot be neglected, as EM geometric similarity is disturbed under its action. Taking this into account, it was obtained that:

$$S_{em} = k_h k_\varphi \ell^{3.5}, \quad (4.2)$$

where k_h, k_φ are coefficients taking the total influence of electromagnetic processes into consideration.

Analogous dependences were obtained for both separate components and total loss power. As a result, relations for calculation of the general exponent n_g and the criterion of the series

optimality K_n were substantiated for the main EM types:

for IM

$$K_{nIM} = \left(\ln \frac{P_{b1}^2 (1 - \eta_{b2})^2 \eta_{m1} \eta_{b1} \cos \varphi_{m1} \cos \varphi_{b2}}{P_{b2}^2 (1 - \eta_{b1})^2 \eta_{m2} \eta_{b2} \cos \varphi_{m2} \cos \varphi_{b1}} \right) / \left(2 \ln \frac{\ell_b}{\ell_m} \right);$$

$$n_{gIM} = \frac{\ln \frac{\sqrt{\eta_m \cos \varphi_m} \sqrt{P_m (1 - \eta_m) \eta_\sigma}}{\sqrt{\eta_b \cos \varphi_b} \sqrt{P_b (1 - \eta_b) \eta_m}}}{\ln(\ell_b / \ell_m)}, \quad (4.3)$$

for DCM

$$K_{nDC} = \left(\ln \frac{P_{b1}^2 (1 - \eta_{b2})^2 \eta_{m1} \eta_{b1}}{P_{b2}^2 (1 - \eta_{b1})^2 \eta_{m2} \eta_{b2}} \right) / \left(2 \ln \frac{\ell_b}{\ell_m} \right);$$

$$n_{gDC} = \left(\ln \frac{P_b (1 - \eta_m)}{P_m (1 - \eta_b)} \right) / \left(2 \ln \frac{\ell_b}{\ell_m} \right), \quad (4.4)$$

for SM

$$K_{nSM} = \left\{ \ln \frac{\left[\frac{P_{b1} (1 - \eta_{b2}) \cos \varphi_{m1} \cos \varphi_{b2}}{P_{b2} (1 - \eta_{b1}) \cos \varphi_{m2} \cos \varphi_{b1}} \right]^2 \eta_{m1} \eta_{b1}}{\eta_{m2} \eta_{b2}} \right\} / \left(2 \ln \frac{\ell_b}{\ell_m} \right);$$

$$n_{gSM} = \left(\ln \frac{P_b (1 - \eta_m) \cos^2 \varphi_m}{P_m (1 - \eta_b) \cos^2 \varphi_b} \right) / \left(2 \ln \frac{\ell_b}{\ell_m} \right). \quad (4.5)$$

Here index b refers to the most powerful device of the series and m to the least powerful one; index 1 denotes the first series and index 2 the second one.

The introduction of these relations makes it possible to fully estimate the technical level of the developed series compared with the existing ones at the design stage and to choose an optimal variant of its improvement.

The results of experimental research of EM of different types and series confirmed the correspondence of the values of electromagnetic and total loss powers indices' dependences on rotation axis height in accordance with the obtained theory.

The possibilities of additional improvement of EM power parameters by:

- application of magnetic excitation, along with electromagnetic excitation, in synchronous machines (SM) and direct current machines (DCM);
- use of an electric field, along with a magnetic field, in the air gap of micromachines of synchronous and asynchronous types were substantiated.

Transformers. Taking into account the influence of current frequency, magnetic field induction in the transformer iron, and current density in its windings made it possible to improve the exponent value in the dependence of electromagnetic power on GLD.

Therefore, m -phase transformer power proved to be proportional to any linear dimension to the fourth degree

$$S \sim \ell^4. \quad (4.6)$$

It follows from (4.3) that transformer linear dimensions increase proportionally to the fourth degree root of power

$$\ell \sim S^{1/4}. \quad (4.7)$$

Voltage u_c of one winding turn is proportional to squared diameter of the rod $d^2 \sim \ell^2$ or

$$u_c \sim S^{1/2}, \quad (4.8)$$

i.e. it grows with the increase of transformer power.

The weight of transformer active materials, steel G_{st} and winding material G_w , grows proportionally to cube of its linear dimensions

$$G \sim \ell^3 \sim S^{3/4}. \quad (4.9)$$

Active material consumption per unit of transformer power changes proportionally

$$g = \frac{G}{S} \sim \frac{S^{3/4}}{S} = \frac{1}{S^{1/4}}, \quad (4.10)$$

i.e. it decreases when power grows. Loss $\sum \Delta P_i$ in core steel and windings active materials are proportional to their masses or volumes, when electromagnetic loads remain unchanged, consequently, overall loss

$$\sum \Delta P_i \sim S^{3/4}$$

or

$$\sum \Delta P_i = k_p \ell^3, \quad (4.11)$$

where k_p is proportionality coefficient.

Loss per power unit

$$\Delta p_i = \frac{\sum \Delta P_i}{S} \sim \frac{1}{S^{1/4}}, \quad (4.12)$$

reduces when transformer power grows, which results in its efficiency increase, accordingly.

The transformer surface, cooled by air or another medium, grows proportionally to its linear dimensions squared

$$S_c \sim \ell^2 \sim S^{1/2},$$

Loss q , ascribed to a unit of cooled surface, also grows

$$q \sim \frac{P}{S_c} \sim \frac{S^{3/4}}{S^{1/2}} = S^{1/4}. \quad (4.13)$$

Dependences (4.6) and (4.12) show that increase of transformer unit power is economically sound, as it results in reduction of specific material consumption per 1 kW of power and improved efficiency. At the same time, it follows from expression (4.13) that the natural growth of a transformer-cooled surface is slower than its loss growth; consequently, the higher the transformer power is, the more difficult the solution of its cooling problem is.

Concerning high voltage transformers, due to specific requirements to insulation gaps, the necessity of dividing GLD into two parts, depending on power and depending on voltage, has been substantiated.

As dependences in transformer power and mass on GLD determined according to power transformer tank dimensions do not meet the known theoretical limits, an approach to the separation of overall dimensions of a transformer active part has been offered. It consists in the use of expressions obtained in an experimental way and connecting GLD ℓ with GLD ℓ_t , determined according to the transformer tank (case), for transformers of various powers.

Furthermore, the necessity of taking into account the change of transformer electromagnetic loads with the GLD increase has been substantiated.

Calculation of GLD according to the transformer active part made it possible to obtain mean values of exponent dependence on ℓ for power, mass and loss power equal to 4,08; 2,98; and 2,89, respectively, which is quite close to the theoretically calculated values.

The magnetic induction in the transformer core is practically unchanged when GLD grows, and the current density in winding of geometrically similar transformers is inversely proportional to square root of linear dimension. Therefore, taking into account the influence of current frequency, the induction of magnetic field in the transformer core and current density in its windings makes it possible to further improve the exponent value in the dependence of electromagnetic power on GLD.

As a result, a criterion for the rational choice for particular models of equal power transformers has been offered. It is based on comparison of a generalised index, taking into consideration the general exponent n_g and exponent n_s showing dependence of power and losses on GLD:

$$n = n_g + \frac{4}{3}n_s. \quad (4.14)$$

The coefficient (4/3) is a relation of theoretic exponents of power S and loss $\sum \Delta P_i$ dependence on GLD.

The character of generalised index change reflects the rationality of the choice of transformer series and enables their comparison only using the known geometric dimensions.

Electric devices. As to ED, the possibility of obtaining all of their electromagnetic and power characteristics from their published data and drawings, as well as by direct measurement without complicated theoretical calculation, has been considered, [5].

ED types, most commonly used in industry, have been considered: internal and external disconnectors, oil big-volume circuit breakers, electromagnetic relays, automatic circuit breakers and fuses. Dependences of the main functional parameters (throughput power, power loss, voltage, tractive effort, power loss coefficient) on GLD have been researched for different ED depending on their function.

Dependences of the contact pressure effort on the generalised linear dimension have been obtained for single-point and multi-point contacts at their plastic and elastic deformation under the condition of constant temperature at the contact point.

The expediency of application of multi-point contacts with plastic deformation (exponent lower values) for high-current contacts and single-point contact with elastic deformation (exponent higher values) for feeble-current contacts has been theoretically confirmed.

It has been determined that the currency density for ED windings with natural convection cooling does not practically depend on GLD, while for contacts under the condition of constant temperature excess, it must be inversely proportional to square root of GLD.

It has been proved that the tractive effort of a series of correctly designed geometrically similar electromagnets used in electromagnetic relays is proportional to the cube of generalised linear dimension. The force calculated in accordance with this condition is sufficient for the drive of the corresponding relay contact mechanism. In this case, the work done by the magnet at the moment of activation is proportional to the fourth-fifth power of GLD.

Introducing a power loss coefficient has been suggested, making it possible to compare, in terms of power, commutation and protective ED in the wide range of their parameters, changing in physically understandable and short form.

The necessity of taking heat removal measures when contact designs are calculated and their overall dimensions increased has been substantiated. A decrease of current density with an exponent exceeding 0.5 can be an alternative. It is necessary to apply electrodynamic compensators, beginning from a certain overall dimension, to make up for arising repulsive force in contacts, which grow when ED dimensions increase.

It has been proved that exponents of ED power parameters dependence on GLD may differ from theoretical values. However, the curves reflecting these dependences asymptotically approach theoretical values.

The theoretical assumption about the primary influence of the power on the overall dimensions has been confirmed for low voltage ED: electromagnetic relays, safety devices and circuit breakers. In this case, the exponent of power dependence of low voltage ED on GLD approaches three. In high voltage ED (such as disconnectors and isolating switches) the overall dimensions, along with power, are greatly influenced by the value of voltage whose exponent of dependence on GLD approaches one.

Experimental research of ED power parameters dependences on the generalised linear dimension has resulted in confirmation of the validity of the given theoretical statements and obtained analytical expressions for the criteria of rational choice of ED and their series.

An index of specific power per mass unit was introduced with the aim of determining the criterion of rational ED choice

$$S_{pM} = S / M , \quad (4.15)$$

where S is the total ED throughput; M is the ED mass.

Moreover, the introduction of two additional values necessary for comparison of devices from two different series has been substantiated:

- total throughput S ; exponent n_S reflecting the change of this power depending on ℓ ;
- power loss coefficient γ (PLC) characterising the amount of power necessary for ED functions and defined as relation between loss power in ED and its input power or throughput;
- exponent n_γ reflecting change of PLC depending on ℓ ; index of specific power per mass unit S_{pM} and index $n_{SM} = n_S - n_M$.

Here, n_M is an exponent characterising change of ED mass depending on GLD.

When the analytical expression for ED rational choice criterion taking these values into account was obtained, the calculation of their weight indices was made.

The coefficient k_p of proportionality reflecting dependence of power P on ℓ was chosen as a power loss weight index. As energy corresponding to this power is lost irreversibly in different ED types.

Weight coefficient k_S of the throughput power is determined as the product of the device averaged efficiency and its averaged power coefficient

$$k_S = \eta_a \cos \varphi_a . \quad (4.16)$$

The practical independence of this index on current type has been proved.

Weight index k_{pM} of specific power per mass unit can be found as relation of averaged cost C_{MS} of specific mass per 1 kW of throughput power to total cost C_{eS} of electric power throughput by ED during the period T of its operation without overhaul.

Averaged cost C_{MS} of a specific mass is determined as relation of cost C_A of ED to throughput power $C_{MS} = C_A / S$.

Thus,

$$k_{pM} = \frac{C_{MS}}{C_{eS}} = \frac{C_A}{STC_e} , \quad (4.17)$$

where C_e is electric power cost.

A minimal relation of the total expenditure to the cost of throughput electric power during ED life time has been offered to be considered as a criterion of a rational choice of a separate ED:

$$k_{OI} = \gamma / k_S + k_{pM} \rightarrow \min . \quad (4.18)$$

The first summand in (15) presents power loss in ED taking the weight index into consideration without connection to its operation time, as losses in ED exist in practically any operating condition. The second summand is connected with ED life time and may change depending on it, as it presents a relative initial expenditure. The offered criterion is techno-economic, as the first summand is determined by technical indices.

To determine a criterion of ED series rational choice, analogously to EM, a general exponent was introduced

$$n_g = 0,8n_S - n_p - k_{pM}n_M , \quad (4.19)$$

where n_p – exponent reflecting ED power change depending on GLD.

In this exponent, the third summand is by several orders less than two first ones, but it can be of a significant importance for the choice of ED series in case of the proximity of these two summands.

When comparing the general exponents of two series having different range boundaries, changes of power, loss and mass, these differences are taken into account by the following indices:

$$n_{SO} = \frac{\ln \frac{S_{b1}S_{m2}}{S_{m1}S_{b2}}}{\ln \frac{\ell_{b1}\ell_{m2}}{\ell_{m1}\ell_{b2}}}; n_{pO} = \frac{\ln \frac{P_{b1}P_{m2}}{P_{m1}P_{b2}}}{\ln \frac{\ell_{b1}\ell_{m2}}{\ell_{m1}\ell_{b2}}}; n_{MO} = \frac{\ln \frac{M_{b1}M_{m2}}{M_{m1}M_{b2}}}{\ln \frac{\ell_{b1}\ell_{m2}}{\ell_{m1}\ell_{b2}}}.$$

Finally, the techno-economic criterion of the rational choice of the first ED series in relation to the second one is of the form:

$$k_{OC} = n_{g1} - n_{g2} - 0,8n_{SO} - n_{pO} - k_{pM}n_{MO} = 0,8(n_{S1} - n_{S2} + n_{SO}) - n_{p1} + n_{p2} - n_{pO} - k_{pM}(n_{M1} - n_{M2} + n_{MO}). \tag{4.20}$$

If indices $n_{S1}, n_{S2}, n_{S3}, n_{S4}$ differ significantly, index k_{pM} can be neglected due to its small value. In this case, the rational choice criterion simplifies, becomes merely technical and assumes the following form after transformations:

$$k_{SO} \approx \frac{\ln \left[\left(\frac{S_{b1}}{S_{m1}} \right)^{0,8} \left(\frac{P_{m1}}{P_{b1}} \right) \right]}{\ln \frac{\ell_{b1}}{\ell_{m1}}} - \frac{\ln \left[\left(\frac{S_{b2}}{S_{m2}} \right)^{0,8} \left(\frac{P_{m2}}{P_{b2}} \right) \right]}{\ln \frac{\ell_{b2}}{\ell_{m2}}} + \frac{\ln \left[\left(\frac{S_{b1}S_{m2}}{S_{m1}S_{b2}} \right)^{0,8} \left(\frac{P_{m1}P_{b2}}{P_{b1}P_{m2}} \right) \right]}{\ln \frac{\ell_{b1}\ell_{m2}}{\ell_{m1}\ell_{b2}}}.$$

If it is difficult or impossible to determine power loss coefficient due to absence of corresponding published technical data of the compared ED, one can use a partial criterion of rational choice, i.e. to analyze only the throughput power

$$k_{SO} \approx \frac{\ln \frac{S_{b1}}{S_{M1}} - \ln \frac{S_{b2}}{S_{M2}}}{\ln \frac{\ell_{b1}}{\ell_{M1}} - \ln \frac{\ell_{b2}}{\ell_{M2}}} + \frac{\ln \frac{S_{b1}S_{M2}}{S_{M1}S_{b2}}}{\ln \frac{\ell_{b1}\ell_{M2}}{\ell_{M1}\ell_{b2}}}.$$

The application of the offered choice criteria shows their efficiency for both choice of separate ED and their series, which makes it possible to compare the techno-economical level of the considered ED only on the basis of the published data: overall dimensions and mass.

5 CONCLUSIONS

1. Previously obtained dependences connecting power and electromagnetic parameters of EM, transformers and ED of different power and series with their geometric dimensions have been generalised.
2. The conditions of choice of EM, transformers and ED, independent of peculiarities of their design, without direct comparison of their electromagnetic and power parameters and characteristics have been substantiated.

References

- [1] **A.I. Voldek:** *Electric machines: Course for Universities*. 3rd edition, revised. L: Energy, P. 95–99. 1978. (in Russian)
- [2] **M.R. Harris, P.J. Lowrenson, J.M. Stefenson:** *Per-unit systems: with special reference to electrical machines*. Cambridge University Press, 1970.
- [3] **A.V. Ivanov-Smolenskii:** *Electrical machines*. MIR Publishers Moscow, Vol. 3, 280 p. 1983.
- [4] **B.I. Nevzlin, M.V. Zagirnyak:** *The expansion of dependences limits of rotating electric machines power parameters on the generalized linear size. Part 1. Specification of dependences of power parameters of rotating electric machines on the generalized linear size*. News of Higher Education Institutions. Electromechanics. № 3, pp. 10–17. 2002. (in Russian)
- [5] **M.V. Zagirnyak, B.I. Nevzlin:** *The functional interrelation of mass-overall and power parameters of transformers. Part 1. The known theoretical and experimental dependences between power, electromagnetic and mass-overall parameters of transformers*. News of Higher Education Institutions. Electromechanics. № 6. pp. 47-52. 2004. (in Russian)
- [6] **M.V. Zagirnyak, B.I. Nevzlin, Y.Y. Dyachenko, M.Z.H. Kavakzeh:** *The functional interrelation of mass-overall and power parameters of electric devices. Part 1. The analysis of known theoretical and experimental dependences between power, electromagnetic and mass-overall parameters of electric devices*. News of Higher Education Institutions. Electromechanics. № 3. pp. 20–26. 2008. (in Russian)

A FUZZY MODEL OF POWER SUPPLY SYSTEM CONTROL

MEHKI MODEL UPRAVLJANJA ENERGETSKEGA SISTEMA

Janez USENIK[✉]

Keywords: power supply system, energy capacities, demand, fuzzy logic, neural net

Abstract

In this article, a mathematical model of control of a dynamic system is described; one such system could be a power supply system. Analytical approaches that have been developed to describe the influence of production and stock, i.e. additional capacities, require a hierarchical spatial pattern and demand. Demand is usually an inherently stochastic process, but in this article we simulate it as an output fuzzy variable in a fuzzy system, in which all the input variables are also fuzzy. Furthermore, an interesting use of neural sets is shown, which is presented as an efficient method for the optimisation of the fuzzy system. At the end, a numerical example is given.

Povzetek

V članku je predstavljen mehki model upravljanja dinamičnega sistema, ki je lahko tudi energetska sistem. Razviti analitični pristopi, s katerimi opišemo medsebojni vpliv proizvodnje ter zalog, v takšnih sistemih so to dodatne kapacitete, zahtevajo hierarhično porazdeljeno prostorsko dogajanje/porabo oziroma povpraševanje. Prikazana je možnost, da povpraševanje, ki je po naravi stohastični proces, simuliramo z mehkim sistemom, kjer so vhodne spremenljivke opisane z mehкими množicami. V nadaljevanju članka pa prikažemo še možnost uporabe nevronske mreže kot izjemno zanimiv in zlasti zelo učinkovit način optimizacije mehkega sistema. Na koncu je narejen tudi numerični izračun.

[✉] Corresponding author: Prof. Janez USENIK, PhD., University of Maribor, Faculty of Energy Technology, tel. +386 31 751 203, Fax: +386 7 620 2222, Mailing address: Hočevarjev trg 1, 8270 Krško, e-mail address: janez.usenik@uni-mb.si

1 DEFINING THE PROBLEM

A model of optimal control is determined by a system, input/output variables and the optimal criterion function. The system represents a regulation circle, which generally consists of a regulator, a control process, a feed-back loop, and input and output information. In this article, we will discuss a dynamic system, see Fig. 1, Usenik, [1], in which the input variable is fuzzy. The optimality criterion is the optimal and synchronized balancing of planned and actual output functions.

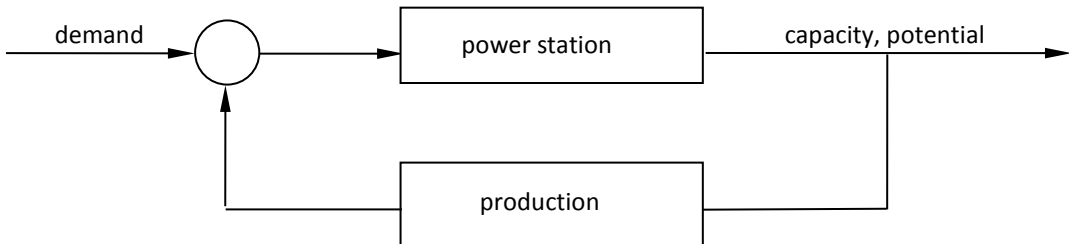


Figure1: Regulation circuit of the power supply system

Let us consider a production model in a linear stationary dynamic system in which the input variables indicate the demand for products manufactured by a company. These variables, i.e. the demand in this case, can be a one-dimensional or multi-dimensional vector function, or deterministic, stochastic or fuzzy.

When the demand is a stochastic process, the task is to determine the optimum production and capacities, so that the total cost will be as low as possible. From Usenik, [1], it is known that the solution of this task is given by the Wiener-Hopf equation. In the special case in which the autocorrelation function of demand is known in the form $R_{dd}(\tau) = e^{-|\tau|}$, we obtain

$$u_{opt}(t) = \frac{1}{1-A} \left[\frac{C-A}{A} e^{-\frac{t}{A}} + (1-C)e^{-t} \right] \tag{1.1}$$

$$v(t) = u(t-\lambda) = \frac{(A-C)}{(1-A)} e^{-\frac{(t-\lambda)}{A}} - \frac{C-1}{A-1} e^{-(t-\lambda)} \tag{1.2}$$

$$D(t) = 1 - e^{-t} \tag{1.3}$$

$$Z_{opt}(t) = M \left[e^{-\frac{(t-\lambda)}{A}} - Ke^{-t} \right] \tag{1.4}$$

λ - lead time

$$K = -\frac{C-1}{A-1} e^\lambda \quad M = \frac{C-A}{A-1} \quad C = \frac{1+A-e^{-\lambda}}{1+A} \quad A = \frac{K_u}{K_z}$$

K_z and K_u are positive constant factors, attributing greater or smaller weights to individual costs. Both factors have been determined empirically for the every product, Usenik, Bogataj, [2], [3].

In this article, we will research only the demand as fuzzy variable and given by fuzzy inference system.

2 FUZZY MODEL

2.1 Fuzzy logic and fuzzy reasoning

Fuzzy logic is a technology that allows a description of the desired system behaviour by using spoken language. Many successful applications are achieved not by conventional mathematical modelling but with fuzzy logic, Altrock, [4]. Fuzzy logic allows that something is not only 'true' or 'false', it allows for partial or multi-valued truths. This discipline is especially useful for problems that cannot be simply represented by classical mathematical modelling due to either the data being incomplete or the process perhaps being too complex. Statements using subjective categories have a major role in the decision making process of people. These statements perhaps do not have quantitative contents; they are perhaps uncertain, imprecise or ambiguous, but people can use them successfully for complex evaluations.

Fuzzy logic is operating with terms such as 'fuzzy set', 'fuzzy variable', 'fuzzy number', 'fuzzy relation' and so on. Fuzzy sets are always functions that map a universe of objects onto the unit interval $[0, 1]$. The degree of membership in a fuzzy set A becomes the degree of truth or a statement and is expressed by continuous membership function.

The combination of imprecise logic rules in a single control strategy is called approximate or fuzzy reasoning (inference). Thus, the fuzzy inference is the process of formulating the mapping from a given input to an output using fuzzy logic.

The output of a fuzzy process can be the logical union of two or more fuzzy membership functions defined on the universe of discourse of the output variable. Defuzzification is the conversion of a given fuzzy quantity to a precise crisp quantity. At least seven methods, Ross, [5], in the literature are popular for defuzzifying given fuzzy output membership functions: max-membership principle, centroid method, weighted average method, mean-max membership, centre of sums, centre of largest area, first (last) of maxima. Several computer programs used ones and some the others. Our model is created by software FuzzyTech 5.55i, and we use defuzzification method called Centre of Maximum (CoM).

In principle, every system can be modelled, analysed and solved by means of fuzzy logic. Due to the complexity of the given problem and the subjective decisions of customers, which are better described with fuzzy reasoning, it is advisable to introduce a fuzzy approach. Some basic solutions of the control problems using fuzzy reasoning were presented in the papers of Usenik, Bogataj, [2], [3]. For some problems about the control of the power supply system, we propose fuzzy reasoning. It is obvious that decision makers, when solving everyday problems in the control of systems, operate with fuzzy logic, Zimmerman, [6].

2.2 Fuzzy system

Construction of a fuzzy system takes several steps: selection of decision variables and their fuzzification, establishing the goal and the construction of algorithm (base of rules of fuzzy

reasoning), inference and defuzzification of the results of fuzzy inference. A graphic presentation of a fuzzy system is given in Figure 2, Vizinger, Usenik, [7].

The entire system demonstrates the course of inference from input variables against output and it is built on a base of 'if-then' fuzzy rules. The fuzzy inference consists of three phases:

1. Fuzzification
2. Fuzzy inference
3. Defuzzification

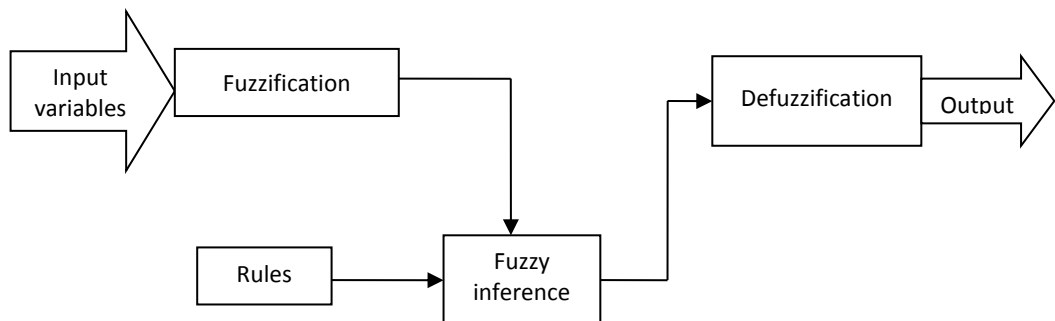


Figure 2: Elements of fuzzy system

2.2.1 Fuzzification

In the fuzzification phase, we have to define fuzzy sets for all fuzzy variables (input and output) and define their membership functions.

Let us assume that the demand d_i at the location z_j depends on a) the market area, b) the density of the area, c) price, d) season and d) uncertainty. The demand is in fact the basic variable, on which the behaviour of all retailers depends.

We assume that all expressions are fuzzy variables, market area, density of the area, price, season and uncertainty are input fuzzy variable, and demand is an output fuzzy variable (Fig. 3).

Every fuzzy variable is presented by more terms:

- a) The input fuzzy variable MARKET AREA is represented by: SMALL, BIG;
- b) The input fuzzy variable DENSITY OF THE AREA is represented by: WEAK, MEDIUM, STRONG;
- c) The input fuzzy variable PRICE is represented by: LOW, MEDIUM, HIGH;
- d) The input fuzzy variable SEASON is represented by: LOW, HIGH;
- e) The input fuzzy variable UNCERTAINTY is represented by: SMALL, MEDIUM, BIG, VERY_BIG;
- f) The output fuzzy variable DEMAND is represented by: VERY_LOW, LOW, MEDIUM, HIGH, EXTREMELY_HIGH.

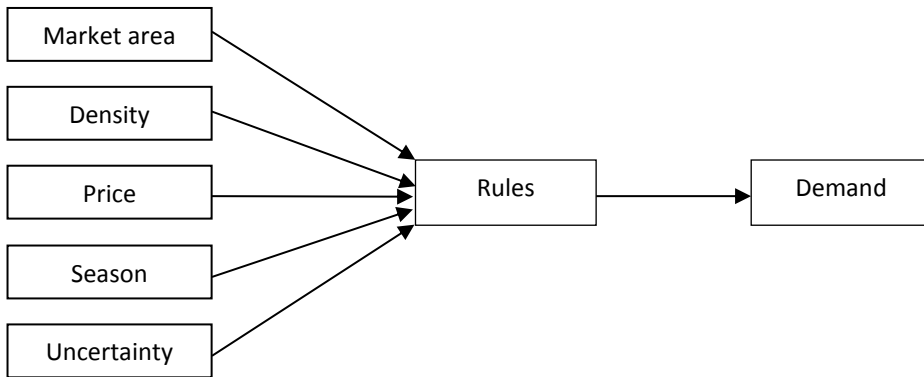


Figure 3: The output fuzzy variable ‘demand’ depends on 5 input fuzzy variables

For every fuzzy set and for every fuzzy variable, we have to create membership functions, see Figures 4-9.

On the x-axis, we measure the variables MARKET AREA, DENSITY,.... , DEMAND are given in units such as number of customers, Euro/kWh, MWh and so on, depending on our data. On the y-axis, we measure membership for every possible fuzzy variable and for every fuzzy set.

Due to the simplicity in this model, we suppose that all units for all fuzzy variables are given in relative measure, i.e. percentages from 0 to 100. Of course, the expert knows what, for example, 30% for ‘market area’ or 80% of the ‘price’ etc. mean.

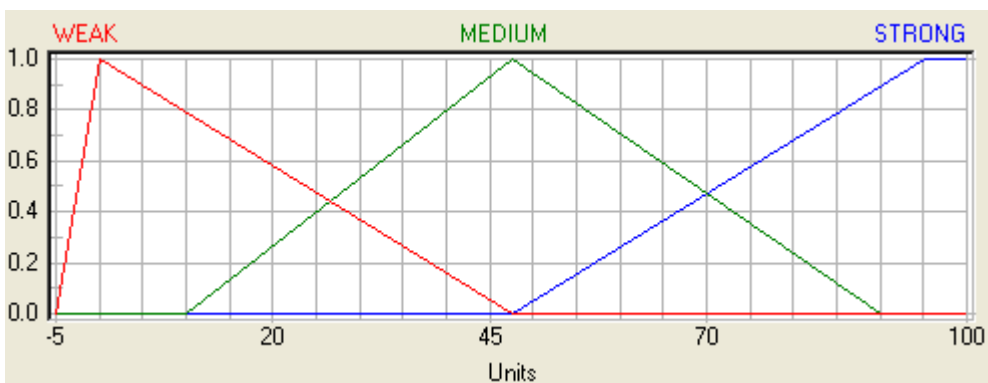


Figure 4: Memberships functions of fuzzy sets for fuzzy variable DENSITY

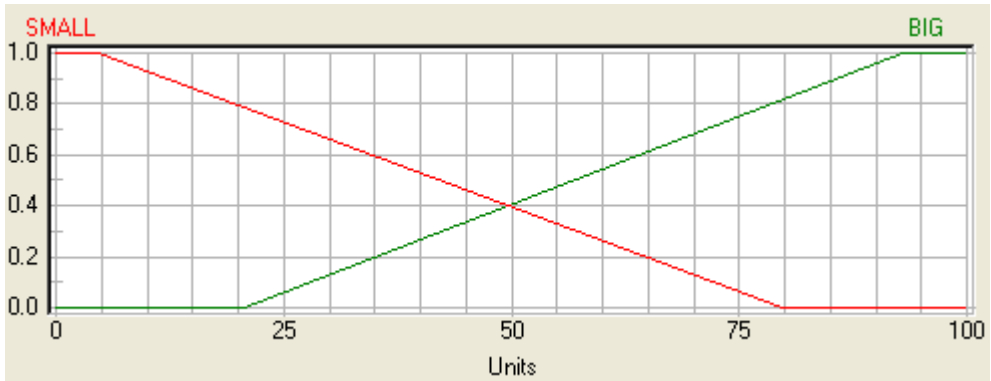


Figure 5: Memberships functions of fuzzy sets for fuzzy variable MARKET



Figure 6: Memberships functions of fuzzy sets for fuzzy variable PRICE

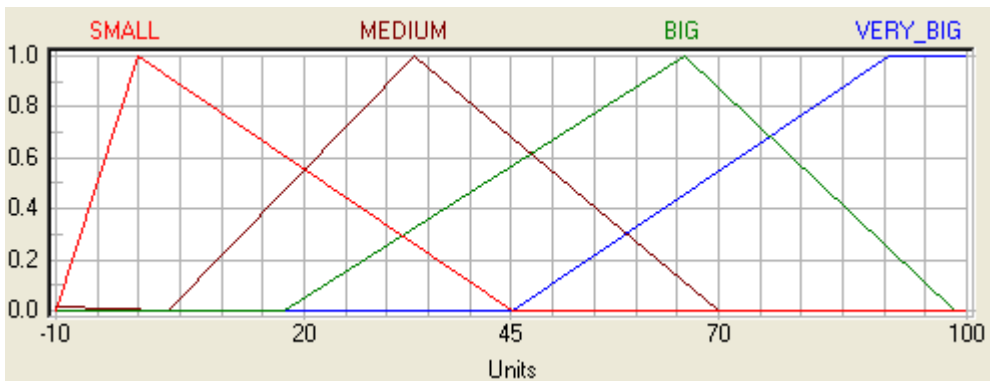


Figure 7: Memberships functions of fuzzy sets for fuzzy variable UNCERTAINTY

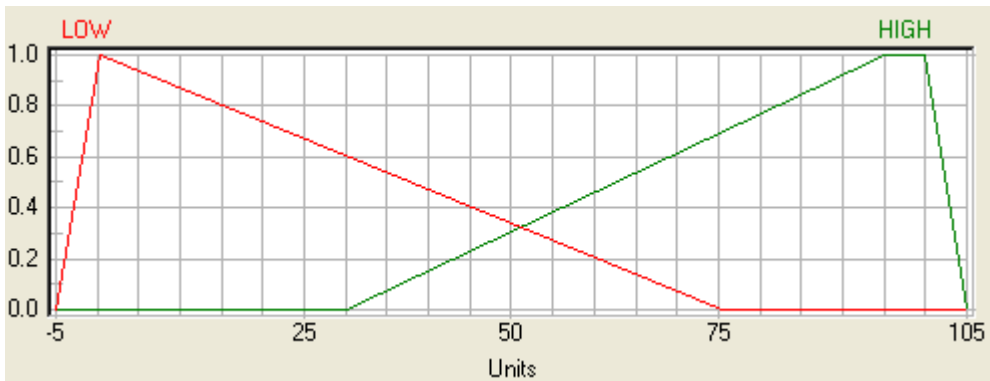


Figure 8: Memberships functions of fuzzy sets for fuzzy variable SEASON

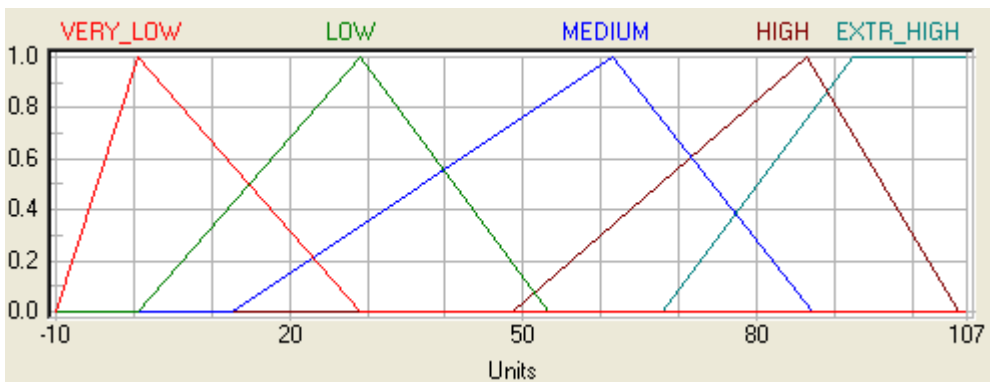


Figure 9: Memberships functions of fuzzy sets for fuzzy variable DEMAND

2.2.2 Fuzzy rules inference

Fuzzy inference is a process in which a certain conclusion/decision is derived from a set of fuzzy statements.

In addition to linguistic variables, there are basic widgets of a fuzzy logic system as well as sets of rules that define the behaviour of system. A single fuzzy rule (implication) assumes the form: **if x is A then y is B** , where A and B are linguistic values defined by fuzzy sets on the universes of discourse X and Y , respectively. The *if* part of the rule is called the antecedent or premise, while the *then* part is called the consequent or conclusion. Variables x and y are defined on the sets X and Y .

With the assembly of a base of rules, the question always appears of how to obtain the rules. Usually this is written down as a base of knowledge within the shape of 'if-then' rules by an expert for a definite system based on his own knowledge and experiences. An expert must also define entry and exit fuzzy functions, their shape and position. However, it often occurs that his knowledge is not sufficient and he cannot define an adequate number of rules. Therefore, the procedures of forming or supplementation to the base of rules based on available numerical data were developed, Vizinger, Usenik, [7].

With fuzzy inference, we must put all values and facts in a definite order and connect them to the procedure of inference execution, so that will be feasible with a computer. This order is given as a list or system of rules, Table 1.

In our work, we applied FuzzyTech software (FuzzyTech, 2001). In accordance of this software tool, 144 rules were automatically created.

Table 1: Some rules for fuzzy model 'demand'

IF						THEN
density	market	price	season	uncertainty	DoS	demand
WEAK	SMALL	MEDIUM	LOW	BIG	1.00	LOW
WEAK	SMALL	MEDIUM	HIGH	BIG	1.00	LOW
WEAK	SMALL	HIGH	LOW	MEDIUM	1.00	VERY_LOW
WEAK	BIG	LOW	HIGH	BIG	1.00	HIGH
WEAK	BIG	MEDIUM	HIGH	BIG	1.00	MEDIUM
MEDIUM	SMALL	MEDIUM	LOW	BIG	1.00	LOW
MEDIUM	BIG	MEDIUM	HIGH	SMALL	1.00	MEDIUM
STRONG	SMALL	MEDIUM	HIGH	BIG	1.00	MEDIUM
STRONG	BIG	MEDIUM	HIGH	MEDIUM	1.00	HIGH
STRONG	BIG	HIGH	HIGH	MEDIUM	1.00	HIGH
STRONG	BIG	MEDIUM	HIGH	VERY_BIG	1.00	EXTR_HIGH

In Table 1, the first five columns represents input fuzzy variables, the last column is output fuzzy variable and the sixth column DoS is 'degree of support' (also 'rule weight'), this is degree to which a rule is valid or plausible, FuzzyTech, [8].

2.2.3 Defuzzification

The result from the evaluation of fuzzy rules is fuzzy. Defuzzification is the conversion of a given fuzzy quantity to a precise crisp quantity. In procedure of defuzzification, fuzzy output variables are changed into crisp numerical values. There are many procedures for defuzzification, which give different results.

The most frequently method used in praxis is CoM defuzzification (the Centre of Maximum). As more than one output term can be accepted as valid, the defuzzification method should be a compromise between different results. The CoM method does this by computing the crisp output as a weighted average of the term membership maxima, weighted by the inference results, Ross, [5]. CoM is a type of compromise between the aggregated results of different terms j of a linguistic output variable and is based on the maximum Y_j of each term j .

As already mentioned, there are many methods of defuzzification that generally give various results. In our example, our model is created by software FuzzyTech 5.55i, and we use the Centre of Maximum (CoM) defuzzification method.

2.3 Optimisation

When the system structure is set and all elements of the system are defined, the model must also be tested and checked for its fit to data and for producing the desired results. However, in our case, we have tasks with relatively simple optimization, because we have limited the problem to concrete conditions. We simplified the system so that it is well defined and gives the desired results. During optimization, we are verifying the entire definition area of input data.

For each point of the definition area, we check whether the system is giving the desired result and if this result is logical. If we are not satisfied with the results, we can change any of the membership functions or any of fuzzy inference rules.

For optimisation we have some different methods, such as trial and error, or using graphic tools, which can visually demonstrate system activity. Such a graphic demonstration shows us the response to a change of data or change in definition of the system elements, FuzzyTech, [8].

One of the most efficient methods is using neural nets during the neuro-fuzzy training to obtain good and regular results.

2.4 About neural net

Artificial neural networks, or simply 'neural networks', Hagan, [9] are a new generation of information systems that demonstrate the ability to learn, recall and generalize from training patterns (data). Artificial neural networks are constructed to make use of some principles resembling the human brain. These nets use a number of simple computational units called neurons, each of which tries to imitate the behaviour of a single human brain cell. The human brain contains approximately 10^{11} nerve cells with approximately 10^{14} mutual connections. Each neuron has an activation level that ranges between a maximum and a minimum. A typical neuron has three major parts: a cell body, dendrites and an axon. The end of an axon splits into strands; each strand terminates in a small bulblike organ called a synapse where the neuron passes its signal to the neighbouring neurons. There are approximately 10^4 synapses per neuron in a human brain. The signals reaching synapses and received by dendrites are electric impulses. The receiving cell fires if its electric potential reaches a threshold, and an action potential of fixed strength and duration is sent out through the axon to synaptic junctions of other neurons.

Based on this explanation of the human neuron, a model of the neuron was made (Figure 10). The input signals x_1, x_2, \dots, x_n representing the output signals of other neurons, are all weighted by corresponding elements (weights) w_1, w_2, \dots, w_n . Each weight corresponds to the strength of a biological synaptic connection. The neuron has a bias b added to the weighted inputs to the output $n = w_1x_1 + w_2x_2 + \dots + w_nx_n + b$, called net input (*NET*) or propagation function, Hagan, [9], Dreyfus, [10] and others. The net input goes into a transfer (or activation) function f , which produces the neuron output $y = f(w_1x_1 + w_2x_2 + \dots + w_nx_n + b)$, see Figure 10.

The activation function can be linear or nonlinear function of n . A particular activation function is chosen to satisfy a specification of the problem that the neuron is attempting to solve. The most commonly used activation functions are a step function, a sigmoid function, a hyperbolic-tangent function and an identity function.

The neurons in the neural network operating in parallel are called a layer. The layer includes a weight matrix, a propagation function, a bias vector, activation functions and an output vector.

Each element of the input vector is connected to each neuron through the weight matrix. Each neuron has a bias, a propagation function, an activation function and an output. Let us consider a network with several layers. Each layer has its own weight matrix, its own bias vector, a net input vector and an output vector. A layer whose output is the network output is called an output layer; the other layers are called hidden layers.

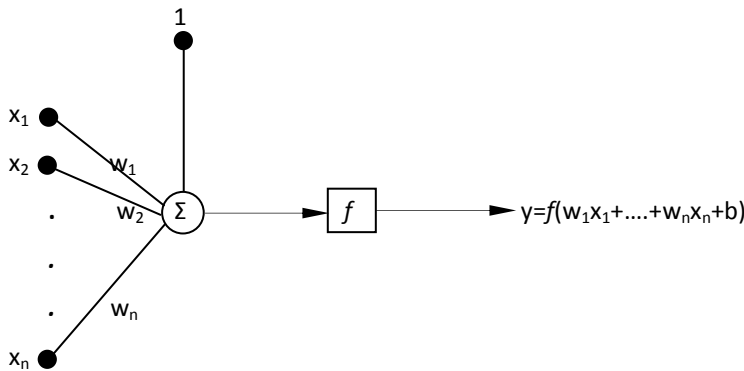


Figure 10: The structure of an artificial multiple-input neuron

The most practical neural networks have two or three layers, Rao, [11]. Depending on the signal transmission through the network, neural networks are with or without feedback. Artificial neural networks with feedback are connections between output and input nodes, and are capable of modifying their behaviour in response to the environment. They can be trained and they can learn; many training algorithms have been developed. The back propagation method is well known and frequently used, including in our work. The main idea of this method is to compare the results computed by the current neural network with the target output value from the sample pattern. The deviation between the values is used to update the net. In the training process we have to follow some steps, Fuzzy Logic Toolbox User's Guide, [12]:

- select samples from a sample data base,
- compute network: the network is fed with input data (forward propagation), the results of the nets computation are retrieved at its output units,
- compare calculated results with the given sample and compute a deviation,
- change net weights in accordance with the computed error,
- back propagation: the net weights are changed by starting from the output neurons stepping backwards through the net up to the input units,
- iterations: the procedure repeats these steps with every data set until the average error is reduced to less than a threshold given in advance.

2.4.1 Neuro-Fuzzy technology

Fuzzy systems and neural networks are both numerical model free estimators and dynamic systems, Lee, [13]. They estimate functions from samples without requiring a mathematical formulation, and learn from them. In the estimation process, fuzzy systems use fuzzy set samples, while neural systems use numerical samples. Neural nets can learn from data sets, while fuzzy logic solutions are easy to verify and optimize. A neural net can learn from data sets;

fuzzy logic requires defining everything explicitly. Knowledge and representation in neural nets are implicit, i.e. the system cannot be easily interpreted or modified, while in fuzzy logic verification and optimization are easy and efficient. The combination of these two technologies makes it possible to use their separate advantages. The synthesis of the explicit knowledge representation of fuzzy logic with the learning ability of neural nets is called NeuroFuzzy. This proposed architecture is referred to as ANFIS (Adaptive NeuroFuzzy Inference System), Young, [14].

NeuroFuzzy has many advantages, FuzzyTech, [8], including:

- the representation of the input and output variables by membership functions and the structure of the information flow in the system already contain much of the information that an unstructured neural net must derive from the sample data set;
- we can use any knowledge about the system from the start;
- we can exclude parts of the system from training;
- we can interpret the results or current stage of the system as it contains self-explanatory fuzzy logic rules and linguistic variables;
- we can manually optimize the results of NeuroFuzzy training;
- we can interactively train our system.

NeuroFuzzy has also some disadvantages:

- this technology is still young and developed by practitioners rather than researchers;
- NeuroFuzzy training features a lower degree of freedom for the learning algorithm when compared to neural nets.

2.4.2 Neurofuzzy training

To optimise our results and to obtain a stable and robust fuzzy model, we have to perform neurofuzzy training. At this point, help from expert who knows the system very well is required. Suppose that we have a base of knowledge and we can start our neurofuzzy procedure; we have used the FuzzyTech software’s option for neuro-fuzzy learning. Making 500 iterations, we have changed the shapes of the membership functions for all fuzzy variables and changed weights (DoS) for some rules for fuzzy inference.

Membership functions after neurofuzzy training are shown in Figures 11–16.

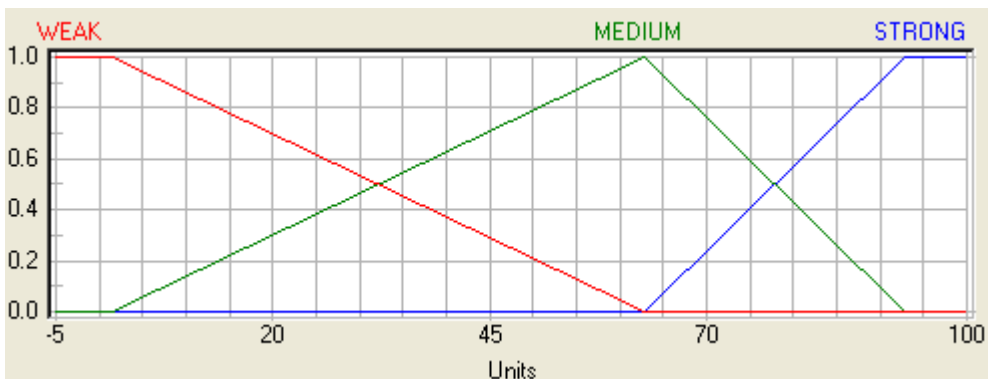


Figure 11: MBF of 'density'



Figure 12: MBF of 'market'



Figure 13: MBF of 'price'



Figure 14: MBF of 'season'



Figure 15: MBF of 'uncertainty'

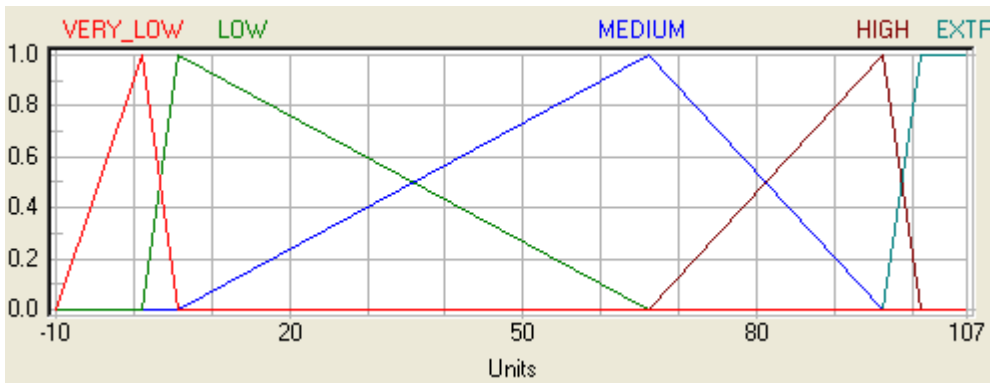


Figure 16: MBF of 'demand'

After 500 iterations, we also changed the weights (DoS) for some rules for fuzzy inference. In Table 2, we can see some rules (the same as in Table 1) with changed weights DoS.

Table 2: Some rules after neurofuzzy training

IF					THEN	
density	market	price	season	uncertainty	DoS	demand
WEAK	SMALL	MEDIUM	LOW	BIG	1.00	LOW
WEAK	SMALL	MEDIUM	HIGH	BIG	0.13	LOW
WEAK	SMALL	HIGH	LOW	MEDIUM	0.64	VERY_LOW
WEAK	BIG	LOW	HIGH	BIG	1.00	HIGH
WEAK	BIG	MEDIUM	HIGH	BIG	0.52	MEDIUM
MEDIUM	SMALL	MEDIUM	LOW	BIG	0.00	LOW
MEDIUM	BIG	MEDIUM	HIGH	SMALL	0.19	MEDIUM
STRONG	SMALL	MEDIUM	HIGH	BIG	1.00	MEDIUM
STRONG	BIG	MEDIUM	HIGH	MEDIUM	0.98	HIGH
STRONG	BIG	HIGH	HIGH	MEDIUM	0.98	HIGH
STRONG	BIG	MEDIUM	HIGH	VERY_BIG	0.73	EXTR_HIGH

3 NUMERICAL RESULTS

Some results are given in Table 3. The first five columns represents input fuzzy variables, the last column 'demand' as output of the fuzzy system is divided in three sub-columns. In the first, we can see crisp values of demand before neurofuzzy training, in the second after neurofuzzy training, and in the third are values from base of knowledge used in procedure of training.

Table 3: Some numerical results

density	market	price	season	uncertainty	demand		
					before	after	sample
0	0	100	0	0	0	1	0
50	50	50	50	50	60	50	50
100	100	1	100	100	100	100	100
30	30	80	80	50	50	42	-
70	50	90	20	90	45	58	-
60	100	40	50	50	77	73	-
60	60	30	50	50	71	67	-
70	70	90	90	70	72	76	-
90	50	100	100	100	74	78	-
50	30	80	20	20	31	28	-
19	33	49	66	66	53	52	57
39	70	60	60	50	52	54	55
78	78	39	78	78	88	80	80

Of course, in Table 3 we merely have some results, but with interactive simulation, which is possible with FuzzyTech software, we can simulate every situation. The quality of the results depends on the expert, who prepares a data file for the neuro-training procedure.

4 CONCLUSIONS

In this article, the fuzzy model of the one part, i.e. demand of the control of the power supply system (see Figure 1) has been presented. Demand is the most important variable for all decisions about activities in a power supply system, such as to build or not build a new power supply plant. In case of fuzzy conditions, demand and other functions were represented as fuzzy sets. In the future, research will have to be done in order to create a mathematical model of the power supply system for fuzzy conditions in general. All variables are inherently fuzzy, especially in the crisis of the global world economy. In our model, we have also so called 'uncertainty' as fuzzy input variable. This can mean many things, e.g. the problem of terrorism, the problem of a lack of natural resources or the problem/costs in buying in carbon credit coupons etc. Research and studying of fuzzy model(s) is important because of the fuzzy nature of the energy market and offer some relevant answers for the future.

References

- [1] **J. Usenik:** *Mathematical model of the power supply system control*, JET Journal of Energy technology, Volume 2 (2009), p.p. 29–46.
- [2] **J. Usenik, M. Bogataj:** *A fuzzy set approach for a location-inventory model*. Transp. technol., 2005, vol. 28, no. 6, pp. 447–464.
- [3] **M. Bogataj, J. Usenik.:** *Fuzzy approach to the spatial games in the total market area*. *Int. j. prod. econ.* [Print ed.], 2005, vol. 93-94, pp. 493–503.
- [4] **C. von Altrock:** *Fuzzy logic&neurofuzzy applications explained*, Prentice Hall, Inc., Englewood Cliffs, NJ 07632, 1995.
- [5] **J. T. Ross:** *Fuzzy Logic with Engineering Applications*, second edition, John Wiley&Sons Ltd,The Atrium, Southern Gate, Chichester, 2004.
- [6] **H. J. Zimmermann:** *Fuzzy Set Theory - and Its Applications*, 4th edition, Kluwer Academic Publishers, Dordrecht, 2001.
- [7] **T. Viziger, J. Usenik.:** *Energy efficient of fuzzy approach in controlling traffic signalization*, JET Journal of Energy technology, Volume 3 (2010), p.p. 49–73.
- [8] *FuzzyTech, Users Manual*, 2001, INFORM GmbH, Inform Software Corporation.
- [9] **M. T. Hagan, H. B. Demuth, M. Beale:** *Neural Network Design*, International Thomson Publishing, PWS Publishing Company, Boston, 1996.
- [10] **G. Dreyfus:** *Neural networks, methodology and applications*, Springer-Verlag Berlin Heidelberg, 2005.
- [11] **A. Rao, J. Srinivas:** *Neural Network, Algorithms and applications*, Alpha Science International Ltd., 2003.
- [12] *Fuzzy Logic Toolbox User's Guide*, For Use with MATLAB, The MathWorks, Inc., 2000.
- [13] **R. S. T- Lee:** *Fuzzy-Neuro Approach to Agent Applications, From AI perspective to modern ontology*, Springer-Verlag Berlin Heidelberg, 2006.
- [14] **J. R. Jang, C. Sun, C., E. Mizutani:** *Neuro-Fuzzy and Soft Computing*, Prentice Hall Inc., Upper Saddle River, NJ 07458, 1997.

FRACTURE TOUGHNESS OF HETEROGENEOUS ENERGY COMPONENTS

LOMNA ŽILAVOST HETEROGENIH ENERGETSKIH KOMPONENT

Zdravko Praunseis^{3†}

Keywords: fracture toughness, energy materials, experimental testing

Abstract

The presence of different microstructures along pre-crack fatigue fronts has important effects on the critical crack tip opening displacement (CTOD). This value is the relevant parameter for the safe servicing of energy components (penstocks). In the case of specimens with a through thickness notch partly in the weld metal, partly in the heat affected zone and partly in the base material, i.e. using the composite notched specimen, the fracture behaviour strongly depends on the portion of ductile base material, its size and the distribution of the mismatching factor along the vicinity of the crack front.

Povzetek

Prisotnost različnih mikrostruktur vzdolž fronte utrujenostne razpoke vpliva na kritično odpiranje konice razpoke (CTOD). Ta vrednost je relevantni parameter za varno obratovanje energetskih component (npr. zapornic hidroelektrarn). V primeru, ko je fronta konice razpoke nameščena po celotni debelini preizkušanca t.i. kompozitna razpoka in je delno prisotna v materialu zvara, toplotno vplivanem področju in osnovnem materialu, takrat je lomno obnašanje materiala odvisno od deleža žilavega osnovnega materiala, velikosti in porazdelitve faktorja trdnostne neenakosti vzdolž fronte konice razpoke.

^{3†} Corresponding author: Zdravko Praunseis, PhD, Faculty of Energy Technology, University of Maribor, Tel.: +386 31 743 753, Fax: +386 7 620 2222, Mailing address: Hočevarjev trg 1, Krško, Slovenia, E-mail address: zdravko.praunseis@uni-mb.si

1 INTRODUCTION

High-strength, low-alloyed (HSLA) steels are often used as materials for penstocks in hydroelectric power stations for the build-up of multi-pass welded joints. The welding of HSLA steels to produce under-matched weld joints presents a technological challenge for the production of modern welded structures.

Under-matched welded joints are used for the repair welding of joint damage due to hard operation conditions or short-period overloading [1]. They are recommended for preventing hydrogen cracking with pre-heating, especially for welded joints made of HSLA steels with yield strengths above 700 MPa.

Crack-tip opening displacement (CTOD) as a fracture toughness parameter is determined as the lowest toughness of different microstructures along the crack front, according to the weakest link model [2–5].

Therefore, the aim of this paper is to analyse the fracture behaviour of HSLA under-matched welded joints made on penstock material, and also to determine the relevant parameters that contribute to higher critical values of fracture toughness [6–8].

2 EXPERIMENTAL PROCEDURE

High-strength low-alloyed (HSLA) steels in a quenched and tempered condition, corresponding to the grade HT 80, were used. The Fluxo-Cored Arc welding process (FCAW) was used and two different tubular wires were selected. Three different types of global under-matched welded joints were produced: one homogeneous and two heterogeneous. The homogeneous welded joint was made with pre-heating and post-heating of the base material, entirely with the same consumable. The two different types of heterogeneous welded joints were made using a softer consumable for the soft root layer: one with two passes and the other with four, in order to avoid preheating of the base material and to prevent cold cracking. Defects in welded joints were detected with non-destructive testing (NDT). Radiography was used, and defects were classified according to the International Standard (IIW).

The basic mechanical properties of multi-pass under-matched joints with homogeneous and heterogeneous welds are obtained using round tensile specimens, extracted from the weld metal in the welding direction, from filler passes and root weld metal region.

In the under-matched joint with homogeneous and heterogeneous welds, in addition to its global strength mismatch between weld metal and base material, there is also a local strength mismatch between the weld metal, HAZ, root weld metal and weld filler metal (filler passes), which is more pronounced for a joint with a soft root layer. Local strength mismatching is especially pronounced in the thickness direction of under-matched joints with homogeneous and heterogeneous welds, which has been determined by micro-hardness measurement (the distance between indents was 1 mm). The strength heterogeneity of the aforementioned welded joint is defined by local mismatching factor ($M=R_{pweld}/R_{pbm}$). To evaluate the weld metal yield strength, an experimental equation ($R_p=3.15HV-168$) is often used [1], employing micro-hardness measured values HV.1 in all joint points. In this way, the strength mismatching factor M in every point of welded joint is roughly determined.

The fracture toughness of homogeneous and heterogeneous under-matched weld joint was evaluated using the standard static CTOD test. The testing temperature was -10°C following the recommendation of the OMAE (Offshore Mechanics and Arctic Engineering) association. For CTOD testing, a single specimen method was used (Fig.1). To evaluate the fracture toughness of under-matched welded joints, standard [2–4] bending specimens ($B \times 2B$, $B=36$ mm) with a deep ($a/W=0.5$) notch in the Heat Affected Zone (HAZ) were used. For all specimens, fatigue pre-cracking was carried out with the GKSS Step-Wise High R ratio method (SHR) procedure. During the CTOD tests, the DC potential drop technique was used for monitoring the stable crack growth. The load line displacement (LLD) was also measured with the reference bar to minimize the effects of possible indentations of the rollers. The CTOD values were calculated in accordance with BS 5762 [2] and also directly measured by GKSS [5] developed δ_5 clip gauge on the specimen side surfaces at the fatigue crack tip-over gage length of 5 mm.

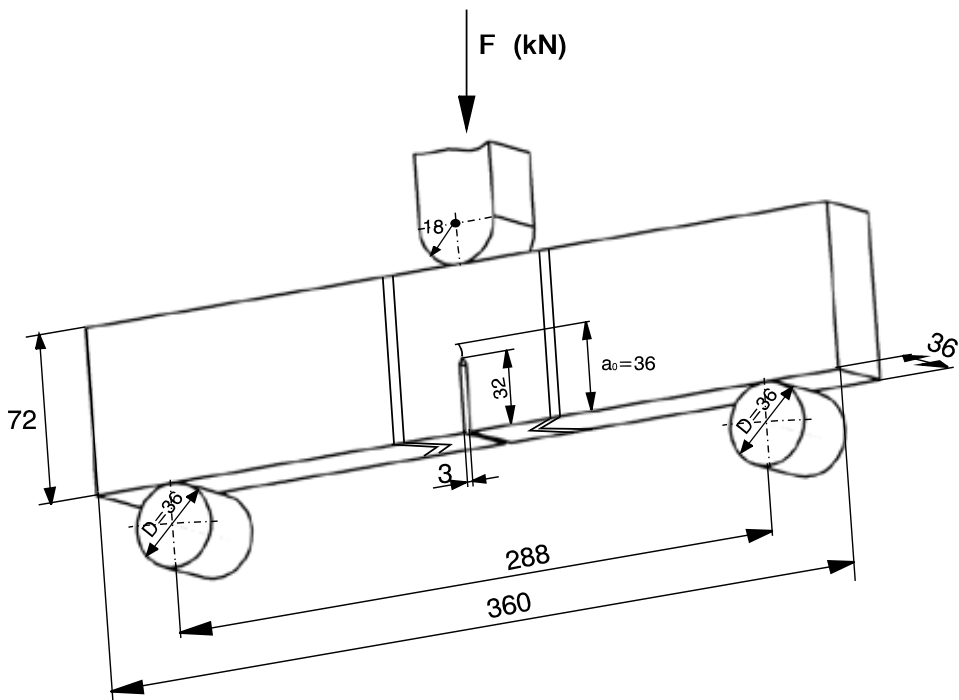
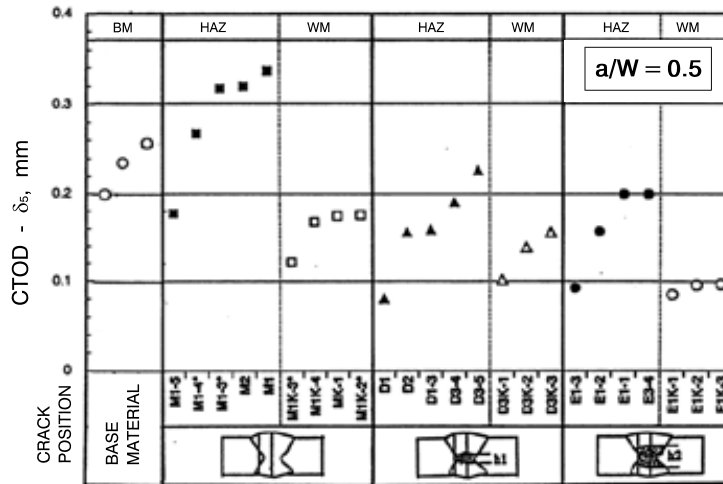


Figure 1: Shape and dimensions, and loading conditions for bend SENB specimens ($B \times 2B$), made from homogeneous and heterogeneous under-matched weld joints

3. RESULTS AND DISCUSSION

HAZ fracture toughness is relatively high; in the case of homogeneous weld, it is much higher than the base material toughness (Fig.2). One of the reasons for high toughness in HAZ was composite fatigue crack front, including a narrow HAZ region with the Coarse Grain (CG) HAZ of extremely low fracture toughness (Local Brittle Zones), but the remaining part, i.e. most of the

fatigue crack front, was contained the tougher weld filler metal, base material and remaining fine grain HAZ (FG HAZ and Inter Critical (IC) HAZ).



*) Non uniform fatigue crack front profile

Figure 2: CTOD (δ_5) fracture toughness values for specimens Bx2B in homogeneous and heterogeneous under-matched weld joints, measured at -10°C

The main reason for this was different root welding heat input energy, causing different widths of HAZ in the root region of homogeneous and heterogeneous weld and consequently affecting initiation of the final brittle fracture of the specimen (Fig.3). Specifically, the distance of fatigue crack tip front from fusion line was approximately the same (≈ 3.5 mm) for the CTOD specimens with soft root layer and without it [1, 6–8].

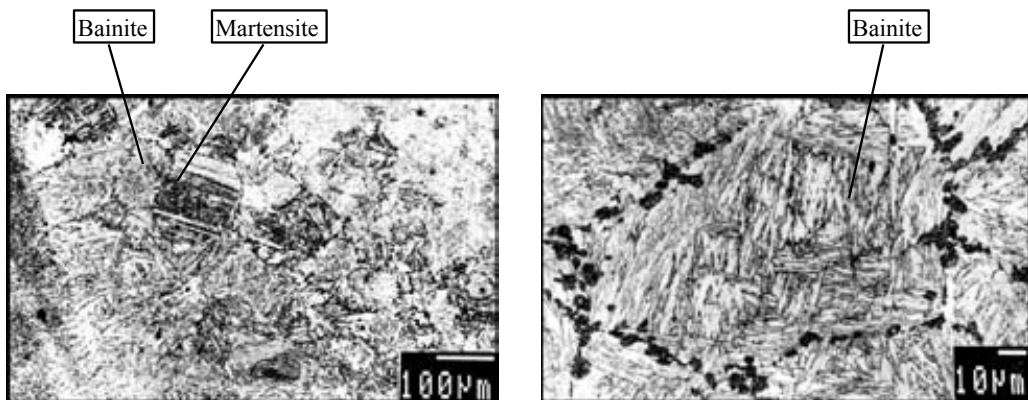


Figure 3: CG HAZ a) with bainitic-martensitic microstructures, which was subsequently heated at temperatures between A_{c1} and A_{c3} , i.e. IC CG HAZ; b) with distributed brittle M-A constituents along grain boundaries of primary grains (ASTM 4) with directed bainitic microstructures.

Apart from that, one must not forget that for the fatigue cracks, CG HAZ of two different widths related to CG HAZ region of different grain sizes were sampled, which partially caused the appearance of brittle fracture origins, influencing the HAZ fracture toughness of both welds.

In CTOD specimens with cracks in the HAZ of homogeneous welds, brittle fracture initiation started in the weld material with the lowest value of mismatch factor M , because of the shielding effect of over-matched root weld metal. The LBZs were recorded during CTOD testing of welded joint as pop-ins (Fig.4). After that, an increase in stress intensification followed in the HAZ, leading to the final brittle fracture of specimen through CG HAZ and the base material, which has provided the least resistance in the specimen centre. The origin of final brittle fracture appeared in the tougher fine grain IC HAZ. The crack path deviated to the softer base material, due to shielding effect of root overmatched weld metal.

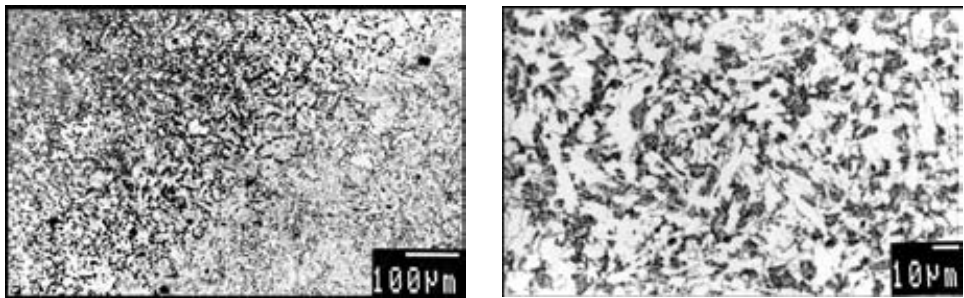


Figure 4: HAZ a) heated at inter-critical temperatures between A_{c1} in A_{c3} (IC HAZ). At higher magnification, b), the region of partial transformation to austenite, from which M-A constituents are formed, can be seen

In the case of CTOD testing of specimens with soft root layers, the first brittle fractures (LBZs) appeared in IC CG HAZ, which were recorded as small pop-ins. Due to high local strength mismatch between the base material and the soft root layer, the crack propagated towards the region of lower toughness, i.e. towards the fusion line and under-matched weld metal. The Fe_3C carbide was identified as the brittle fracture initiation point at the fracture surface, with the use of EDX analysis. The effect of the soft root layer on strain distribution along the fatigue crack front was so pronounced that it caused strain concentrations in the soft root layer. Due to its low toughness, this has initiated the final specimen fracture in coarse grain IC HAZ and crack path deviation towards zone of the soft root layer, with further reduction of toughness level, which would be achieved with higher soft root layer toughness.

The classification of CTOD resistance curves (Fig.5) for specimens with deep cracks in the HAZ confirms the abovementioned analysis and conclusions that the HAZ fracture toughness of homogeneous welds is much higher than that of heterogeneous welds. By increasing the soft root layer thickness, the HAZ fracture toughness of the heterogeneous weld joint reduces and becomes lowest for the welded joint with the four-pass soft root layer, as is clear from the classification of CTOD resistance curves in Fig. 5.

From comparison of calculated (δ_{BS}) and measured (δ_5) CTOD values, a good agreement is obvious, which is especially important in order to verify detailed and directly measured CTOD - δ_5 values, for which one does not need to know the yield strength and the rotation factor as in the case of CTOD - δ_{BS} calculated values.

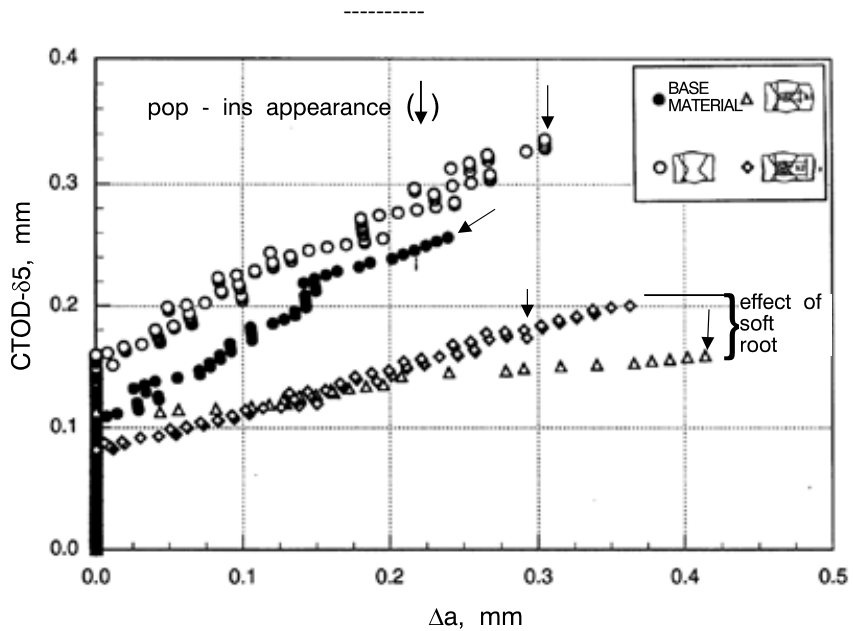


Figure 5: Resistance curves for specimens ($B \times 2B$) with deep crack ($a/W = 0.5$) in the HAZ of homogeneous and heterogeneous under-matched weld joints.

This is very important in cases in which the fatigue crack tip front crosses regions with different strength levels and where the effect of local strength mismatch at the crack tip is significant, as shown for fracture behaviour of under-matched joints with homogeneous and heterogeneous weld metals. More detailed analysis shows that $CTOD-\delta_5$ values are generally lower than $CTOD-\delta_{BS}$ values, thus being more conservative.

4 CONCLUSIONS

The fracture behaviour of specimens notched partly in the HAZ is strongly affected by microstructures at the crack tip. Improvement in HAZ toughness has been achieved due to its widening by higher input energy ($Q +$ preheating) in the root region, so that one part of the fatigue crack tip front passed through the normalized fine grained HAZ region. The HAZ fracture toughness of heterogeneous welds is appreciably lower than the HAZ fracture toughness of homogeneous welds due to low ductility of the soft root layer, which has caused brittle fracture initiation of welded joint by diverting the fracture path from the HAZ to the soft root layer.

Strength mismatch also has a significant influence on the real values of HAZ fracture toughness. Obtained values in both examples are not the real values for HAZ fracture toughness, because they were influenced by properties of weld root strength. Fracture deviation towards the base material (homogeneous weld) overestimates HAZ fracture toughness, whereas fracture deviation towards the soft root layer (heterogeneous weld) underestimates the HAZ fracture toughness. Therefore, HAZ fracture toughness determination is a complex problem that could be solved by synthetic multi-pass microstructures and their fracture toughness.

Acknowledgements

The authors wish to acknowledge the financial support of the Slovenian Foundation of Science and Technology and the Japanese Promotion of Science.

References

- [1] **Praunseis, Z.:** *The influence of Strength Under-matched Weld Metal containing Heterogeneous Regions on Fracture Properties of HSLA Steel Weld Joint* (Dissertation in English). Faculty of Mechanical Engineering, University of Maribor, Slovenia, 1998
- [2] BS 5762, *Methods for crack opening displacement (COD) testing*, The British Standards Institution, London 1979.
- [3] ASTM E 1152-87, *Standard test method for determining J-R curves*, Annual Book of ASTM Standards, Vol. 03.01, American Society for Testing and Materials, Philadelphia, 1990.
- [4] ASTM E 1290-91, *Standard test method for crack-tip opening displacement (CTOD) fracture toughness measurement*, American Society for Testing and Materials, Philadelphia, 1991.
- [5] GKSS Forschungszentrum Geesthacht GMBH, *GKSS-Displacement Gauge Systems for Applications in Fracture Mechanic*.
- [6] **Praunseis, Z., Toyoda, M., Sundararajan, T.:** *Fracture behaviours of fracture toughness testing specimens with metallurgical heterogeneity along crack front*. Steel res., Sep. 2000, 71, no 9,
- [7] **Praunseis, Z., Sundararajan, T., Toyoda, M., Ohata, M.:** *The influence of soft root on fracture behaviors of high-strength, low-alloyed (HSLA) steel weldments*. Mater. manuf. process., 2001, vol. 16, 2
- [8] **Sundararajan, T., Praunseis, Z.:** *The effect of nitrogen-ion implantation on the corrosion resistance of titanium in comparison with oxygen- and argon-ion implantations*. Mater. tehnol., 2004, vol. 38, no. 1/2.

ISENTROPIC EFFICIENCY OF GAS TURBINE AXIAL COMPRESSORS AND THE OUTDOOR TEMPERATURE EFFECT

IZENTROPSKI IZKORISTEK AKSIALNEGA TURBOKOMPRESORJA PLINSKE TURBINE IN VPLIV ZUNANJE TEMPERATURE

Josip Gašparinčič^{3†}, Aleš Štricelj¹

Keywords: Gas turbine, axial turbo compressor, isentropic efficiency, temperature, pressure

Abstract

This paper presents the calculation of the isentropic efficiency of a gas turbine axial compressor manufactured by Alstom. Isentropic efficiency shows how much energy is transformed in exergy and how much into anergy. This paper presents the calculation of axial compressor characteristics of an Alstom GT11N2 thermal power plant in Brestanica, Slovenia. The efficiency changes dependant on external temperatures during 2009 are also presented.

Povzetek

V članku je predstavljen izračun izentropnega izkoristka aksialnega kompresorja plinske turbine proizvajalca Alstom. Izentropski izkoristek prikazuje kolikšen delež energije se spremeni v eksergijo ter kolikšen v anergijo. Članek predstavlja izračun karakteristik aksialnega kompresorja plinske turbine Alstom GT11N2 postavljene v Termoelektrarni Brestanica. V članku je prikazana sprememba izkoristka za različne temperature spremljane skozi celo leto 2009.

^{3†} Corresponding author: Josip Gašparinčič, M.S. Mech. Eng., Termoelektrarna Brestanica d.o.o., Slovenia Tel.: +386 7 481 6303, Fax: +386 7 497 1288, Address: CPB 18, 8280 Brestanica, Slovenia, E-mail address: josip.gasparincic@teb.si

¹ Aleš Štricelj, B.S., Termoelektrarna Brestanica d.o.o., Slovenia, Tel.: +386 7 481 6240, Fax: +386 7 497 1288 Address: CPB 18, 8280 Brestanica, Slovenia, E-mail address: ales.stricelj@teb.si

1 INTRODUCTION

An axial turbo-compressor is a part of an energy turbo-machine. For turbine rotors, there are specially designed turbine blades through which the working substance flows. In gas power plants operating in a simple cycle process the working substance is air. The purpose of a turbo-compressor is that it increases energy with compressed substances in one or more stages. For example, with air it increases density, pressure and temperature, while the specific volume decreases. Therefore, it is necessary to add an axial turbo-compressor, e.g. electrical energy, which is changed into kinetic energy in the blades. For a turbo compressor, higher flow, smaller pressure and higher rotation frequency are significant. The construction and working of a turbo-compressor is similar to that of a turbine pump. In this paper, an analysis of an axial turbo-compressor and various effects of external temperatures and relative air humidity are presented, [1].

2 COMPRESSION PROCESS IN GAS TURBINE

With ideal or reversible processes, exergy remains constant while it decreases with actual or irreversible processes. With decreasing exergy, anergy increases. As a result of the imperfections of machines and friction, all technical processes are irreversible.

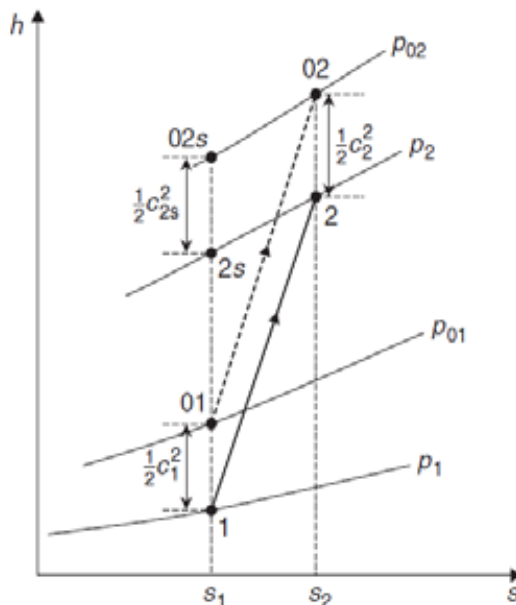


Figure 1: Compression process in axial turbo compressor

The compression process is presented on the h - s diagram in Figure 1. At the beginning, gas is in static condition (1) and stagnation condition (01). At the exit from the defined compressor stage, gas is in static condition (2) and stagnation condition (02). In case that the process is reversible, gas in transition through the turbine stage is in static condition (2s) and stagnation

condition (02s). Line 1-2 represents an irreversible process in static coordinates, while Line 01-02 represents an irreversible process in stagnation coordinates. Each axial turbo-compressor is assembled from a larger number of stages. The isentropic efficiency of an axial turbo-compressor as a whole is always less than the isentropic efficiency of each particular stage, [2],[3].

2.1 Isentropic efficiency of all axial turbo compressor stage especially

The differential increase of pressure is analyzed at one stage in which the change of pressure is displayed with dp .

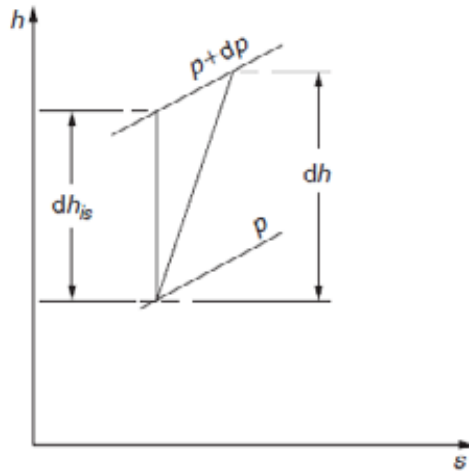


Figure 2: Display of differential reversible and irreversible process in an h - s diagram

With an irreversible process, the differential change of enthalpy is displayed with (dh) and with a reversible process with (dh_{is}) . Isentropic efficiency of one stage is displayed in Eq. (2.1).

$$\eta_p = \frac{dh_{is}}{dh} = \frac{vdp}{C_p dT} \quad (2.1)$$

$$Tds = 0 = dh_{is} - vdp \quad (2.2)$$

Where $dh_{is}=vdp$ results from an equality of heat gain according to the first and second main laws of thermodynamics (2.2). For an ideal gas, (2.3) is valid.

$$v = \frac{RT}{p}, \quad C_p = \frac{\gamma R}{\gamma-1} \quad (2.3)$$

By including (2.3) in (2.1), the following is obtained:

$$\frac{dT}{T} = \frac{(\gamma-1) dp}{\gamma \eta_p p} \quad (2.4)$$

After integration of Eq. (2.4) follows:

$$\frac{T_2}{T_1} = \left(\frac{p_2}{p_1}\right)^{\frac{\gamma-1}{\eta_p \gamma}} \quad (2.5)$$

Whole isentropic efficiency of turbo compressor η_c is:

$$\eta_c = \frac{(T_{2s}-T_1)}{(T_2-T_1)} \quad (2.6)$$

For a reversible process, it is valid that the isentropic efficiency of each stage is $\eta_p = 1$. It follows:

$$\frac{T_{2s}}{T_1} = \left(\frac{p_2}{p_1}\right)^{\frac{\gamma-1}{\gamma}} \quad (2.7)$$

From Eq. (2.7), the next form is given:

$$\frac{p_2}{p_1} = \left(\frac{T_{2s}}{T_1}\right)^{\frac{\gamma}{\gamma-1}} \quad (2.8)$$

Eq. (2.6) is easily transformed in next equation.

$$\eta_c = \frac{(T_{2s}-T_1)}{(T_2-T_1)} = \frac{T_1 \left(\frac{T_{2s}}{T_1} - 1\right)}{T_1 \left(\frac{T_2}{T_1} - 1\right)} = \frac{\frac{T_{2s}}{T_1} - 1}{\frac{T_2}{T_1} - 1} \quad (2.9)$$

With the placing of Eq. (2.5) and (2.7) into Eq. (2.9), the final form of isentropic efficiency calculation of all axial turbo compressor stages is given. Eq. (2.9) shows that the entire isentropic efficiency of an axial turbo-compressor is less than the efficiency of each stage, [4], [5].

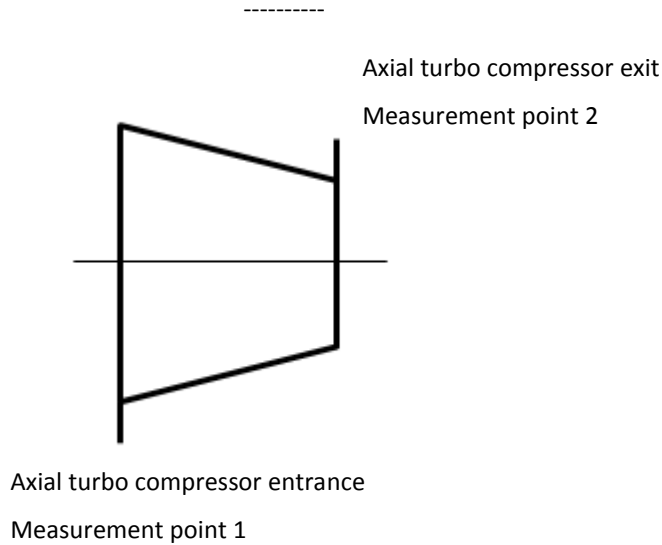


Figure 3: Display of measurement places on axial turbo compressor

3 CALCULATION OF ISENTROPIC EFFICIENCY OF AN ALSTOM GT11N2 GAS TURBINE IN THE BRESTANICA THERMAL POWERPLANT

An Alstom GT11N2 gas turbine has been operating in the Brestanica thermal power plant since the year 2000.

Table 1: Alstom GT11N2 technical data

Technical data GT11N2		
Number of compressor stages		14
Compression ratio		15:1
Combusting chamber type		Vertical
Number of turbine stages		4
Rotor speed		3600 min ⁻¹
Fuel consumption	Nat. gas	33,425 Sm ³ /h
	Oil	29,880 kg/h
Rated power	Nat. gas	108.9 MW
	Oil	114.2 MW
Rated efficiency	Nat. gas	34.0%
	Oil	32.7%

The isentropic efficiency of axial turbo compressor depends on external conditions. This paper presents changes of isentropic efficiency for three various temperatures: $T_1=30^\circ\text{C}$, $T_2=15^\circ\text{C}$ and for $T_3=0^\circ\text{C}$. Input data were collected during the operating of gas turbines in the Brestanica thermal power plant in 2009 from measuring places that are fitted on the turbo-compressor entrance and exit [6], [7], [8].

Table 2: Input data

Date:	19.06.2009	21.10.2009	19.12.2009			
T:	30°C	15°C	0°C			
Humid.	40.25%	58.22%	85.00%			
Rated power	81 MW	107.7 MW	85 MW			
Stage.	p(bar)	T(K)	p(bar)	T(K)	p(bar)	T(K)
Entrance	0.99	303	0.99	283	0.99	273
Exit	11.92	663	14.48	675	13.46	642

3.1 Calculation process

For calculations of complete isentropic efficiency, data on input and output temperatures and pressures are necessary.

From Eq. (2.5) isentropic efficiency of each stage η_p is calculated. By placing Eq. (2.5) and (2.7) into Eq. (2.9), the complete isentropic efficiency of the turbo-compressor is calculated.

$$\eta_{cn} = \frac{\left[\left(\frac{p_n}{p_1} \right)^{\frac{\gamma-1}{\gamma}} - 1 \right]}{\left[\left(\frac{p_n}{p_1} \right)^{\frac{\gamma-1}{\eta_p \gamma}} - 1 \right]} \quad (3.1)$$

It is necessary to define changes of pressure in each stage. It is assumed that the increase of pressure is constant.

The isentropic efficiency of the first stage is defined as η_p , and is equal for each stage. The next stage is added to previous, is first calculated isentropic efficiency from ratio of known pressures. In continuation of calculation by Eq. (3.2), the temperature at the end of each stage is also calculated.

$$T_n = \frac{\left(\frac{p_n}{p_1} \right)^{\frac{\kappa-1}{\kappa}} - 1 + \eta_{cn}}{\eta_{cn}} T_1 \quad (3.2)$$

Temperature results are given in Table 3 and isentropic efficiency results are given in Table 4. The same results are also given in Figures 4 and 5.

From the diagram it is clear that at the higher temperatures, higher isentropic efficiency is reached. However, it is necessary to consider the power attained. First of all, the load of turbine GT11N2 is regulated with burners. When all burners are functioning, the turbine reaches over 60% of rated power.

Further regulation depends of percentage of air flowing through compressor, which is regulated with variable guide vanes and the entrance in turbo compressor.

Table 3: *Temperature changes (T) depending on pressure (p)*

T	30°C		15°C		0°C	
	p(bar)	T(K)	p(bar)	T(K)	p(bar)	T(K)
1	0.99	303	0.99	287	0.99	273
2	1.78	363	1.90	353	1.88	337
3	2.56	407	2.80	400	2.78	382
4	3.33	443	3.71	437	3.67	419
5	4.12	473	4.71	471	4.56	449
6	4.89	500	5.70	501	5.45	477
7	5.67	524	6.69	528	6.34	501
8	6.46	546	7.60	549	7.23	523
9	7.24	566	8.59	571	8.12	544
10	8.02	585	9.59	591	9.01	563
11	8.80	602	10.58	610	9.89	580
12	9.58	619	11.58	628	10.79	597
13	10.36	634	12.57	645	11.68	613
14	11.14	649	13.57	661	12.57	628
15	11.92	663	14.48	675	13.46	642

 Temperature changes depending on pressure in Alstom
 GT11N2 compressor

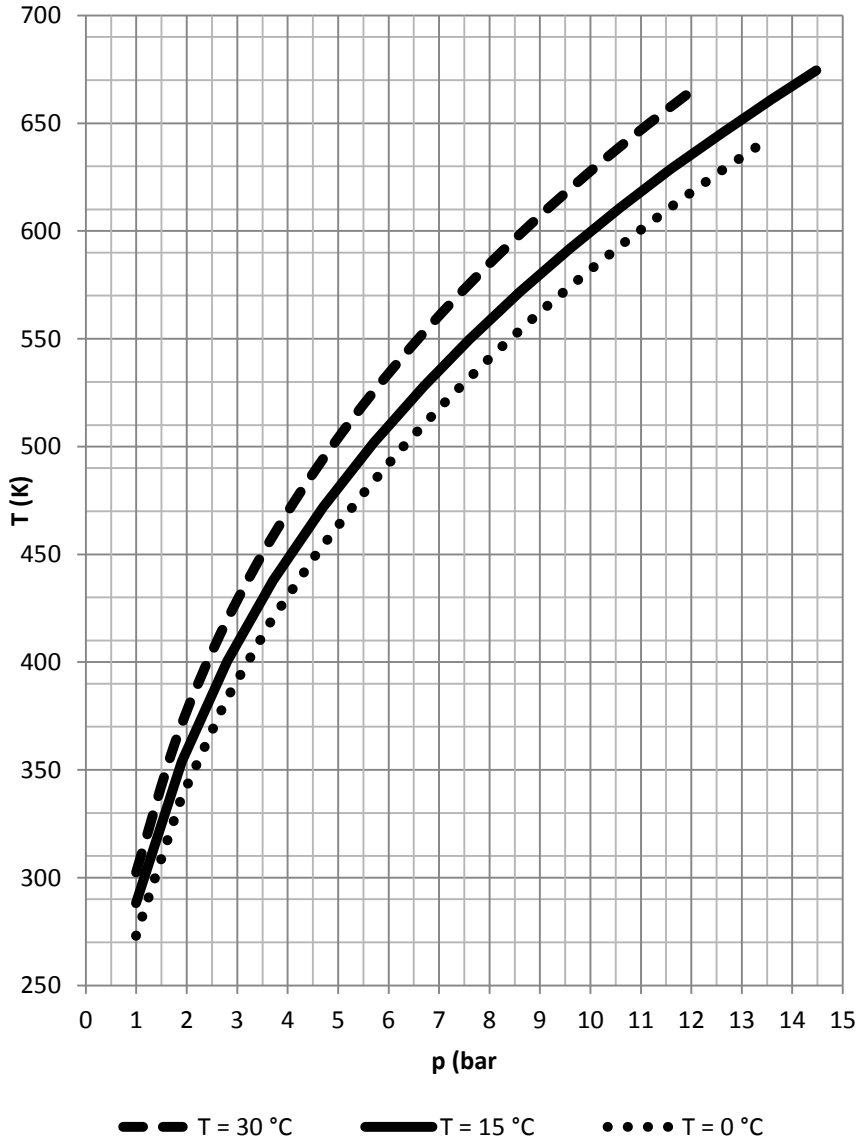


Figure 4: Temperature change (T) depending on pressure (p) in turbo compressor

Table 4: *Decrease of isentropic efficiency at increase of compressor stages*

T	30 °C		15°C		0 °C	
No.	p(bar)	$\eta_c(\%)$	p(bar)	$\eta_c(\%)$	p(bar)	$\eta_c(\%)$
1	0.99	0.903	0.99	0.900	0.99	0.871
2	1.78	0.894	1.90	0.889	1.88	0.859
3	2.56	0.889	2.80	0.884	2.78	0.8511
4	3.33	0.885	3.71	0.880	3.67	0.8455
5	4.12	0.881	4.71	0.876	4.56	0.841
6	4.89	0.879	5.70	0.873	5.45	0.837
7	5.67	0.877	6.69	0.870	6.34	0.834
8	6.46	0.875	7.60	0.868	7.23	0.831
9	7.24	0.873	8.59	0.866	8.12	0.829
10	8.02	0.871	9.59	0.864	9.01	0.827
11	8.80	0.869	10.58	0.862	9.89	0.825
12	9.58	0.868	11.58	0.861	10.79	0.823
13	10.36	0.867	12.57	0.860	11.68	0.821
14	11.14	0.866	13.57	0.858	12.57	0.819
15	11.92	0.865	14.48	0.857	13.46	0.817

Change of isentropic efficiency at Alstom GT11N2 compressor

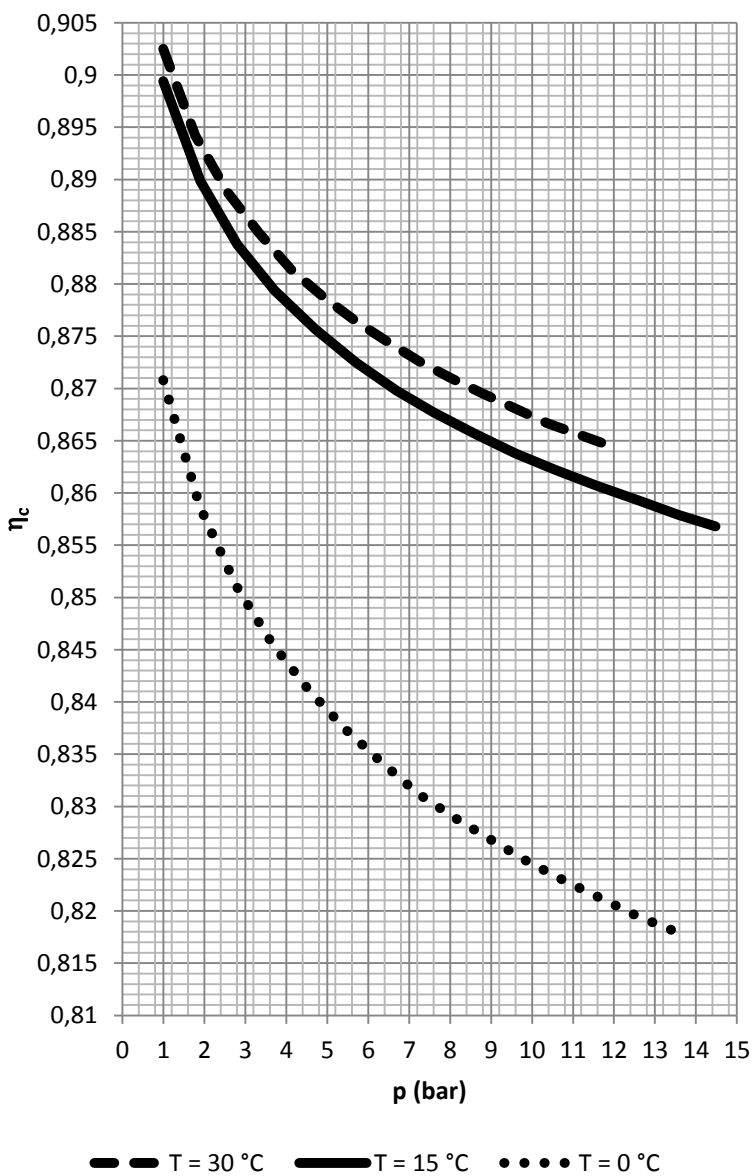


Figure 5: Decrease of isentropic efficiency at increase of compressor stages

4 CONCLUSION

The displayed calculation of isentropic efficiency of an axial turbo-compressor in this paper specifically presents decreases and increases of isentropic efficiency at the entrance of the compressor of an Alstom GT11N2 gas turbine. Furthermore, the power level that is attained during the operating of gas turbine is significant. At the lower attained power levels, but higher entry temperatures and lower relative air humidity, the isentropic efficiency of the entire turbo-compressor is over 86%. This is because the external conditions of dry air and together with lower air supply do not present greater resistance and friction on compressor blades. The most realistic indicator of compressor usage is at a temperature of 15°C and a relative air humidity of 60% (ISO conditions). In this example, the ultimate isentropic efficiency is about 85.7%, which is confirmed by the manufacturer. At the lower temperatures and higher relative air humidity, regardless of the lower attained power levels, isentropic efficiency barely exceeds 81%. Primarily, this is because of higher relative air humidity, which creates great resistance and friction on compressor blades.

References

- [1] **T. Giampaolo:** *Gas Turbine Handbook – Principles and Practice, 4th edition*; 2008
- [2] **S. L. Dixon, C. A. Hall:** *Fluid mechanics and thermodynamics of turbo machinery, 6 Edition Book*; 2010
- [3] **J. H. Horlock:** *Advanced Gas Turbine Cycl, 1st Edition*, 2003
- [4] **M. Tuma, M. Sekavčnik:** *Energetski stroji in naprave – osnove in uporaba*; 2005
- [5] **J. Gašparinčić:** *Razvoj suvremenih energetske postrojenja (Fakultet strojarstva i brodogradnje – Zagreb)*; 2012
- [6] Obratovni podatki TE Brestanica za leto 2010
- [7] Projektna naloga *Garancijske meritve PB4,5 – performance test report Alstom*; 2001
- [8] **I. Kuštrin, M. Sekavčnik:** *TE Brestanica PB5 – enostaven odprt plinski proces*; 2009

RAIN ENERGY AS A GREEN ENERGY SOURCE?

DEŽ KOT ZELENI ENERGETSKI VIR?

Andrej Predin¹, Gorazd Hren²

Keywords: Rain, energy potential of rain, monsoon rain;

Abstract

This paper focuses on using rain as a potential energy source in areas of monsoon rain. On the basis of physical considerations, taking into account the basic laws of mechanics, fluid mechanics and aero-dynamics, the idea of exploiting rain as a green source for energy production is developed. The energy-poor areas of Asia could take advantage of heavy rain during periods of monsoons. From the commercial point of view, this energy source is not profitable, but bearing in mind the underdevelopment of those areas, this energy source could be sufficient for the primary energy supply of individual residential houses.

Povzetek

V prispevku je obravnavana ideja koriščenja dežja kot možnega energetskega vira na področjih monsunskega dežja. Na osnovi fizikalnih opažanj, upoštevajoč osnovne zakone mehanike fluidov in aero-dinamike, je predstavljena ideja o koriščenju dežja kot zelenega energetskega vira. Na področju revnih azijskih držav in tudi širše na monsunskem področju, bi bilo teoretično možno izkoristiti monsunski dež za ceneno pridobivanje električne energije. Iz komercialnega vidika ta vir ne predstavlja profitabilnega vira, vendar pa bi lahko bil na energetske nerazvitih območjih ta vir zanimiv na področju kritja energetskih potreb individualnih stanovanjskih hiš.

¹ Full Professor Andrej Predin, Ph.D., Faculty of Energy Technology, University of Maribor

² Assistant Professor Gorazd Hren, Ph.D., Faculty of Energy Technology, University of Maribor

1 INTRODUCTION

Worldwide demand for energy is projected to increase steadily for the foreseeable future. Fortunately, there are many means of harnessing energy that have less damaging impacts on our environment and are available almost anywhere on Earth. Such alternative energy sources became an issue in the early 1970s when oil prices increased considerably and we were faced with supply shortages. At present, we are facing an ominous reality: the world's energy needs are greater than ever before, driven by an increase of population worldwide, and the industrial and economic development of Asian countries. Furthermore, we are facing demanding and highly increased oil-based energy while the world supply is decreasing. Practically since the year 2000, the world has been facing a permanent increase of oil prices and, consequently, has been searching for new energy resources and exploiting technologies that are efficient and environmentally acceptable. Putting a price on carbon emissions and developing green energy sources are the recommendations for sustainable development included in a report by Kintisch [1]. His conclusions suggest that the urgency of the problem will make up for its lack of originality in seizing the attention of policymakers around the globe, and they intend to launch a major effort to spread the message.

As mentioned in Inter-Academy Council (IAC) report [1] in Amsterdam, the Netherlands, it is a moral and social imperative to meet the basic energy needs of the poorest people on this planet. The developed areas of global academic community are obligated to find and develop green sustainable energy technologies that will help to mitigate basic energy needs in the poorest regions. Could the monsoon rain be such an alternative and green energy source? As Jagadis Sjukla reports in [2], there are some areas in the Indian subcontinent, or more widely in the Asia, where up to 16 mm of rain per square meter per hour were observed during monsoon periods between 2003 and 2006.

2 ENERGY ESTIMATION OF THE RAIN FLOW

The available energy of the rain can be practically estimated in two ways. First, rain could be treated as a flow of the individual water drops, using classic Newtonian mechanical theory. Second, rain could be treated as a two-phase flow and presented with Euler's theory of a velocity field in a vertical direction, considering the earth's gravity.

With Newton's classic mechanical theory, the energy of water drops could be estimated. A raindrop falls from clouds at 2500 m above sea level (ASL) with an approximate mass of 1 gram per individual drop. When the water drop forms, it is spherical. During the fall, the drop is transformed into the more aerodynamic rain-drop shape. Because it starts with free fall, this means from the regular acceleration movement, the differential equation of such movement could be written as:

$$a = \frac{dV}{dt} = \frac{d^2s}{dt^2} = \text{const.} \quad (2.1)$$

Where V is velocity, t is time, and s is distance (path). Equation (2.1) has a solution for free fall cases, in the following form

$$V = \sqrt{2gH} \quad (2.2)$$

in which g is the earth's acceleration coefficient (9.81 m/s^2) and h is the height from which the water drop falls.

Equation (2.2) is suitable only if the exact height (path) is known, and the air drag is neglected. In our case, the drag force is highly influential on drop velocity, and must be considered.

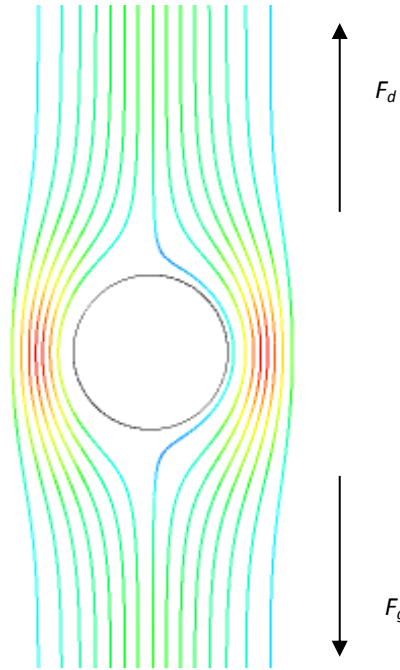


Figure 1: Forces on raindrop.

A raindrop (Figure 1), treated as a falling object, reaches terminal velocity when the downward force of gravity (F_g) equals the upward force of drag (F_d). The net force on the raindrop is zero, resulting into a constant drop velocity. Mathematically, an object (a raindrop in our case) asymptotically approaches and can never reach its terminal velocity. When the object accelerates (usually downwards, due to gravity), the drag force acting on the object increases. At a particular velocity, the drag force produced will equal the object's weight (mg). Terminal velocity (also called settling velocity) varies directly with the ratio of drag to weight. Greater drag means a lower terminal velocity, while increased weight means a higher terminal velocity. The raindrop's weight directly depends on drop size that is formed at different rain types. In the case of a raindrop, it is possible that the drop is moving downward with greater than terminal velocity, because the drop usually changes its shape (into a more aerodynamic form), which is affected by a downward force, or it falls from a thinner part of the atmosphere.

Mathematically, the resulting force is reached when the downward force of gravity (F_g) equals the upward force of drag (F_d), (valid for Reynolds numbers, i.e. $Re > 105$)

$$F = F_g - F_d, \quad (2.3)$$

$$F = mg - C_d A \rho v^2, \quad (2.4)$$

where C_d is the coefficient of the air resistance (drag coefficient), A is project cross-section perpendicular to the drop direction, and p_k is kinetic flow pressure at the stagnation point on a spherical surface, m is the mass of the raindrop (object), and g is the acceleration due to gravity. Dynamic pressure at the stagnation point on the sphere, known also as dynamic pressure, could be written as

$$p_k = \frac{1}{2}\rho V^2, \tag{2.5}$$

Where ρ is the fluid density (e.g. density of air). The terminal velocity is reached when $F = 0$, so

$$mg - p_k A c_d = 0 = mg - \frac{1}{2}\rho V^2 A c_d . \tag{2.6}$$

Solving for V to obtain the expression for the terminal velocity, we obtain

$$V_t = \sqrt{\frac{mg}{\rho A c_d}} . \tag{2.7}$$

With the evaluation coefficient C_d of aerodynamic resistance, considering the form of a sphere and/or drop for the $Re > 105$, we can calculate the terminal velocity of raindrops for different diameters, having assessed the level from which the drop could fall (reach) to the ground (without dividing). Using equation (2.7), the terminal raindrop velocity could be calculated for different drop sizes and different rain types. The results are given in Table 1.

Table 1: Typical drop sizes and its terminal velocities, [3]

RAIN TYPE	Drop Size [mm]	Terminal Velocity [m/s]
Light Stratiform Rain (1 mm per hour)		
Small Drop	0.5	2.06
Large Drop	2.0	6.49
Moderate Stratiform Rain (6.4 mm per hour)		
Small Drop	1.0	4.03
Large Drop	2.6	7.57
Heavy Thundershower (25.4 mm per hour)		
Small Drop	1.2	4.64
Large Drop	4.0	8.83
Largest Possible Drop	5.0	9.09
Hailstone	10	10.00
Hailstone	40	20.00

The energy estimation of raindrops is presented in Table 2.

Table 2: Available energy of raindrops

RAIN TYPE	Drop Size [mm]	Available kinetic energy of one drop [J]	Available kinetic energy at m ² in one hour [J/m ² {hour}]	Available power at m ² [W]/m ²
Light Stratiform Rain (1 mm per hour)				
Small Drop	0.5	2.77E-07	4.24	0.0012
Large Drop	2.0	1.76E-04	42.08	0.0117
Moderate Stratiform Rain (6.4 mm per hour)				
Small Drop	1.0	8.50E-06	103.84	0.1844
Large Drop	2.6	5.27E-04	366.38	0.6507
Heavy Thundershower (25.4 mm per hour)				
Small Drop	1.2	1.95E-05	546.30	3.8506
Large Drop	4.0	2.61E-03	1978.43	13.9450
Largest Possible Drop	5.0	5.40E-03	2096.65	14.7783

If we consider Jagadis Sjukla's report, [2], there are some areas in India or more widely in Asia where up to 16 mm of water per square meter per hour were observed during monsoon season, which corresponds between "Moderate Stratiform Rain" and "Heavy Thundershower" with large drops (Table 1). This means that approximately 10 W of power per square meter is available, in such regions during monsoon rain. If we compare this estimation with wind energy potential, then this energy source is very low from a commercial point of view. Regardless, some small buildings could be adopted with wind turbines. A wind turbine with diameter of 15 m, with efficiency of approximately 0.4, could produce approximately 0.8 kW. This power installation could fulfill the basic household energy needs for lightening and simple heating systems during the long and dark days of monsoon rains.

3 CONCLUSION

With efforts to maximize the use of renewable energy sources, the idea of exploiting the energy of monsoon rain is interesting, especially as an independent and widespread source. The fundamental problem of minimum energy supply could be solved locally in monsoon areas. Currently available technology would be very affordable and suitable to use in economically poor, monsoon areas of Asia. With appropriate international support, it would be possible to provide the local population with enough energy for basic needs such as lighting and heating homes.

References

- [1] **Eli Kintisch:** *Energy policy: National Academies Make Case for Sustainable Growth.* (With reporting by Richard Stone in Beijing), SCIENCE, VOL 318, 26 October 2007, p. 547.

- [2] **Jagadish Shukla:** Atmosphere: Monsoon Mysteries. SCIENCE, VOL 318, 12 October 2007, p.p. 204 -205.
- [3] SUMMARY TABLE - Typical Raindrop Sizes
<http://www.shorstmeyer.com/wxfaq/float/rhtable.html> (Sources: R.R. Rogers, *A Short Course in Cloud Physics*, 2 ed. Pergamon Press, 1979, H. Byers, *General Meteorology*, 3 ed. McGraw-Hill, 1959, H.R. Pruppacher, *Microstructure of Atmospheric Clouds and Precipitation in Clouds: Their Formation, Optical Properties and Effects*, P. Hobbs and A. Deepak, eds., Academic Press, 1981.), Access date: April, 5 2010.

MATHEMATICAL MODELS FOR THE SIMULATION OF PUMPS SYSTEMS

MATEMATIČNI MODELI ZA SIMULACIJO ČRPALNIH SISTEMOV

Mitja Kastrevc^{3†}, Edvard Detiček¹

Keywords: Induction motors, mathematical modelling, hydraulic pump systems

Abstract

This paper presents the influence of a mathematical model in the simulation of pumping systems; specifically, a model of an induction motor is presented; the paper also covers a comparison between commonly used mathematical models of AC motors.

For verification of the simulated data, a practical pump system was tested.

Povzetek

Prispevek obravnava vpliv matematičnega modela na obnašanje črpalnega sistema. Podrobneje je predstavljen model asinhronskega motorja. Prikazuje primerjavo različnih simulacijskih modelov obnašanja asinhronskega motorja

Za potrditev modela je bil izveden eksperimentalni preizkus.

^{3†} Asst. Prof. Mitja Kastrevc, PhD., University of Maribor, Faculty of Mechanical Engineering, Tel.: +386 2 2207804, Fax: +386 2 220 7990, Mailing address: mitja.kastrevc@uni-mb.si

¹ Asst. Prof. Edvard Detiček, PhD., University of Maribor, Faculty of Mechanical Engineering, Tel.: +386 2 2207612, Fax: +386 2 220 7990, Mailing address: mitja.kastrevc@uni-mb.si

1 INTRODUCTION

Trends for the lowering of costs and amount of applied energy on hydraulic power supplies require the use of cost efficient components. Therefore, a combination of an external gear pump and frequency-controlled induction motor is appropriate.

A combination of knowledge in the field of induction motors control drives, external gear pumps and modern control techniques in the field of pressure control is used to improve the dynamic behaviour of supplies' pressure.

This paper presents investigations of descriptions of the dynamic behaviour of such systems. Different mathematical models of an AC motor are used in simulation models to demonstrate differences between them. For the verification of the chosen mathematical model, a comparison between simulated and measured data was made. Therefore, a whole system, including a detailed mathematical model of the induction motor, pipe system and different types of consumers, was used. For comparison with experimental model, the output supply pressure control was also used with the simulation model as with the experimental model.

In the experiment and simulations, the worst case scenarios were investigated. A comparison of results obtained confirms the mathematical models used in the simulations and the selection of the pressure controller type.

2 SIMPLIFIED MATHEMATICAL MODELS OF INDUCTION MOTORS

Setting the rotational speed of induction motors (common in recent times) is primarily done by changing the excitation frequency provided by the inverter. The user often needs to select the speed control mode for several possible implementations provided from inverters.

Describing the engine model was mainly subordinate to the potential performance capabilities of computer-simulations. For a description of both AC and DC machines, a simplified model was used. Various studies indicate models based on this basis. The model that describes the operation of the induction motor is shown in Figure 1 [3].

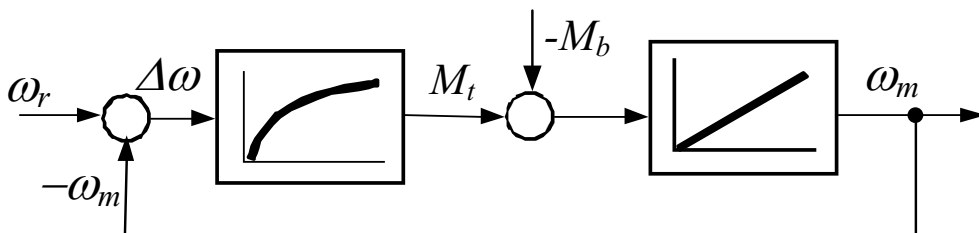


Figure 1: Block diagram of the simulation model of the induction motor

This model allows the simulation that meets the approximate operation of the motor itself, but it can only be used around the nominal operating point of the motor. The constants of the individual transfer functions can be determined using catalogue data.

On the basis of the replacement schematic, shown in Figure 2, we can write the transfer function of the linearized mathematical model outside the nominal operating point [3].

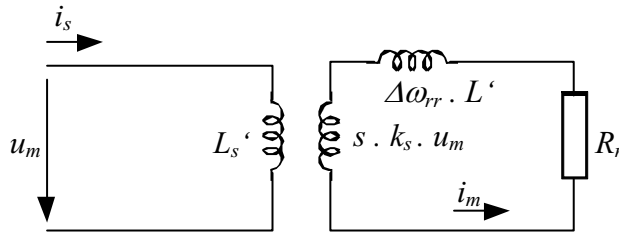


Figure 2: Replacement Scheme asynchronous motor with squirrel-cage

From replacement schematic, the dynamic behaviour is described:

$$s \cdot k_s \cdot u_m = i_m \cdot R_r + L_r' \cdot \frac{di_m}{dt} \quad (2.1)$$

Using Laplace transforms derived transfer function.

$$\frac{i_m(p)}{u_m(p)} = \frac{s \cdot k_s}{R_r + L_r' p} = \frac{s \cdot k_s}{R_r (1 + p T_r')} \quad (2.2)$$

A similarly derived transfer function is the creation of electro-mechanical torque:

$$\frac{\omega_m(p)}{m_m(p) - m_w(p)} = \frac{1}{p \cdot J_{cel}} \quad (2.3)$$

where represents the J_{cel} sum of own inertia motor and load inertia. By knowing the relationship

$$\frac{m_m(p)}{i_m(p)} = k_m \quad (2.4)$$

we can write the transfer function of the entire system. Figure 3 shows a block diagram of the linearized model description of asynchronous motor.

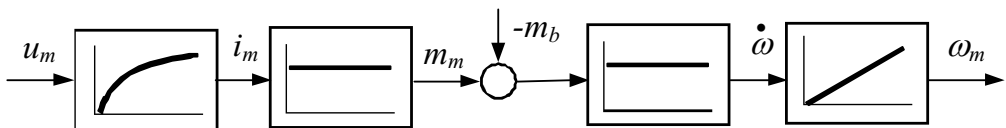


Figure 3: Block diagram of the linearized model of induction motor

To determine the individual constants in the model described above, a test-load (engine, measure voltage, current and power without the connected load) and short circuit (engine at reduced power supply voltage is measured currents of power and torque at locked rotor or

rotor, which rotates with rotational speed $n < 10 \text{ min}^{-1}$) should be carried out. The test may be performed in the laboratory and in industry. Engine manufacturers usually do not give publicise the results of these tests, so users must request the results from the manufacturer or to perform this tests for themselves.

Figure 4 shows the block diagram of the closed-loop model of induction motor suitable for simulation in Matlab-Simulink.

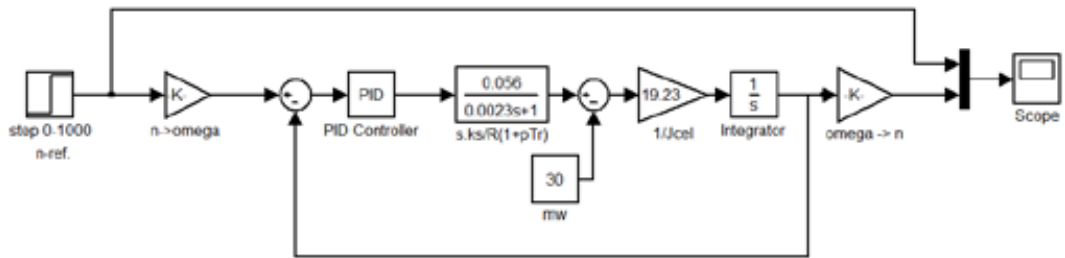


Figure 4: Simulation model of induction motor and frequency controller in a closed control circuit

The disadvantage of such a model lies in the fact that it does not describe the induction motor in the entire operation area; it needs to change simulations often to ignore slip. Thus the engine must be dealt with in the vicinity of the operating point. Often it is necessary to address the phenomena that in the idealised model cannot capture (impact of switching frequencies, outages of individual phases, etc.).

3 DETAILED MATHEMATICAL MODELS OF INDUCTION MOTORS

For the abovementioned reasons, it was necessary to develop a more complete model, which is sufficiently credible to address these phenomena. In the literature [4], [5], we can see different approaches to solving this problem. Common to these sources is using the help of model equations describing the voltage, current situations for stator and rotor, and torque equations. Figure 5 shows an idealized model of three-phase induction motor

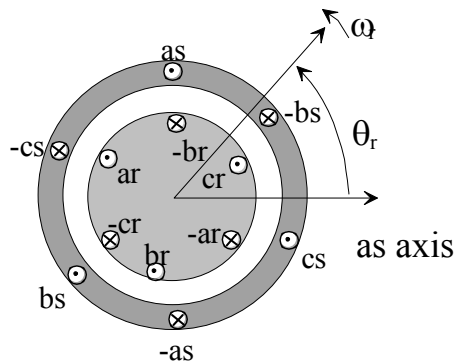


Figure 5: Idealized circuit model of a three-phase induction machine

For the idealized model, we can write the following equation:

$$\begin{aligned}
 v_{as} &= i_{as} \cdot r_s + \frac{d\lambda_{as}}{dt} & [V] \\
 v_{bs} &= i_{bs} \cdot r_s + \frac{d\lambda_{bs}}{dt} & [V] \\
 v_{cs} &= i_{cs} \cdot r_s + \frac{d\lambda_{cs}}{dt} & [V]
 \end{aligned} \tag{3.1}$$

where are v_{as} , v_{bs} , and v_{cs} stator phase voltages, i_{as} , i_{bs} , and i_{cs} stator phase currents and λ_{as} , λ_{bs} and λ_{cs} stator magnetic joints and resistance r_s one phase stator winding.

$$\begin{aligned}
 v_{ar} &= i_{ar} \cdot r_r + \frac{d\lambda_{ar}}{dt} & [V] \\
 v_{br} &= i_{br} \cdot r_r + \frac{d\lambda_{br}}{dt} & [V] \\
 v_{cr} &= i_{cr} \cdot r_r + \frac{d\lambda_{cr}}{dt} & [V]
 \end{aligned} \tag{3.2}$$

where they represent v_{ar} , v_{br} , and v_{cr} rotor phase voltage, i_{ar} , i_{br} , and i_{cr} rotor phase currents and λ_{ar} , λ_{br} and λ_{cr} rotor magnetic conclusions and r_r resistance of one phase of the rotor windings.

$$\begin{aligned}
 T_{em} &= \frac{3}{2} \frac{P}{2} (\lambda'_{qr} i'_{dr} - \lambda'_{dr} i'_{qr}) \\
 &= \frac{3}{2} \frac{P}{2} (\lambda_{ds} i_{qs} - \lambda_{qs} i_{ds}) \\
 &= \frac{3}{2} \frac{P}{2} L (i_{dr} i_{qs} - i_{qr} i_{ds})
 \end{aligned} \tag{3.3}$$

In considering the above, we define a new coordinate system $qd0$; with its help we can treat any operating mode of electric motor (Figure 6).

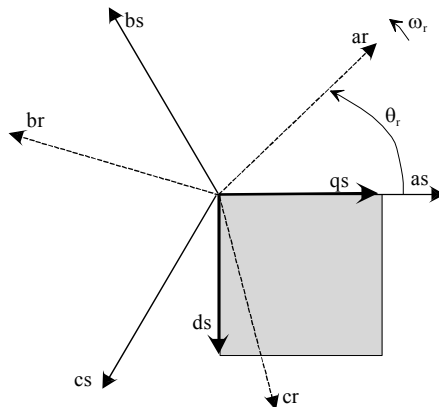


Figure 6: The relationship between the abc coordinate system and the qd0 system

Similar to the *abc* coordinate system, the voltage, current and torque equation for the *qd0* coordinate system can be written:

$$\begin{aligned}v_{qs} &= p\lambda_{qs} + \omega\lambda_{ds} + r_s i_{qs} \\v_{ds} &= p\lambda_{ds} - \omega\lambda_{qs} + r_s i_{ds} \\v_{0s} &= p\lambda_{0s} + r_s i_{0s}\end{aligned}\tag{3.4}$$

$$\begin{aligned}v'_{qr} &= p\lambda'_{qr} + (\omega - \omega_r)\lambda'_{dr} + r'_r i'_{qr} \\v'_{dr} &= p\lambda'_{dr} - (\omega - \omega_r)\lambda'_{qr} + r'_r i'_{dr} \\v'_{0r} &= p\lambda'_{0r} + r'_r i'_{0r}\end{aligned}\tag{3.5}$$

$$\begin{aligned}T_{em} &= \frac{3}{2} \frac{P}{2\omega_r} \left[\omega (\lambda_{ds} i_{qs} - \lambda_{qs} i_{ds}) + (\omega - \omega_r) (\lambda'_{dr} i'_{qr} - \lambda'_{qr} i'_{dr}) \right] \\&= \frac{3}{2} \frac{P}{2} (\lambda'_{qr} i'_{dr} - \lambda'_{dr} i'_{qr}) \\&= \frac{3}{2} \frac{P}{2} (\lambda_{ds} i_{qs} - \lambda_{qs} i_{ds}) \\&= \frac{3}{2} \frac{P}{2} L_m (i'_{dr} i_{qs} - i'_{qr} i_{ds})\end{aligned}\tag{3.6}$$

The next step is, with the help of alternative schemes, to represent Equations 3.4, 3.5 and 3.6. For the simulation, it is necessary to use the correct formulation of these equations in the form of block diagrams.

Modern systems, designed to amend rotational speed induction motors, shall be divided into the so-called scalar and vector systems for setting rotational speed (scalar or vector frequency controllers).

Scalar approaches use changes of stator supply voltage or changes of the slip for setting rotational speed. Their usefulness is mainly reflected in the simplicity and satisfactory usability for less demanding drives, where rotational speed adjustment range is less than the nominal rotational speed.

Vector approaches deal with the ways several parameters change with the greatest impact on the dynamic behaviour of the engine. This can be carried out with the help of voltage, current regulators or regulators with adjustment of the magnetic flux. Also common are systems that contain observers of individual quantities, which would be difficult to measure, and the performance of measurement would be expensive. Figure 7a and 7b show the block diagram of the induction motor.

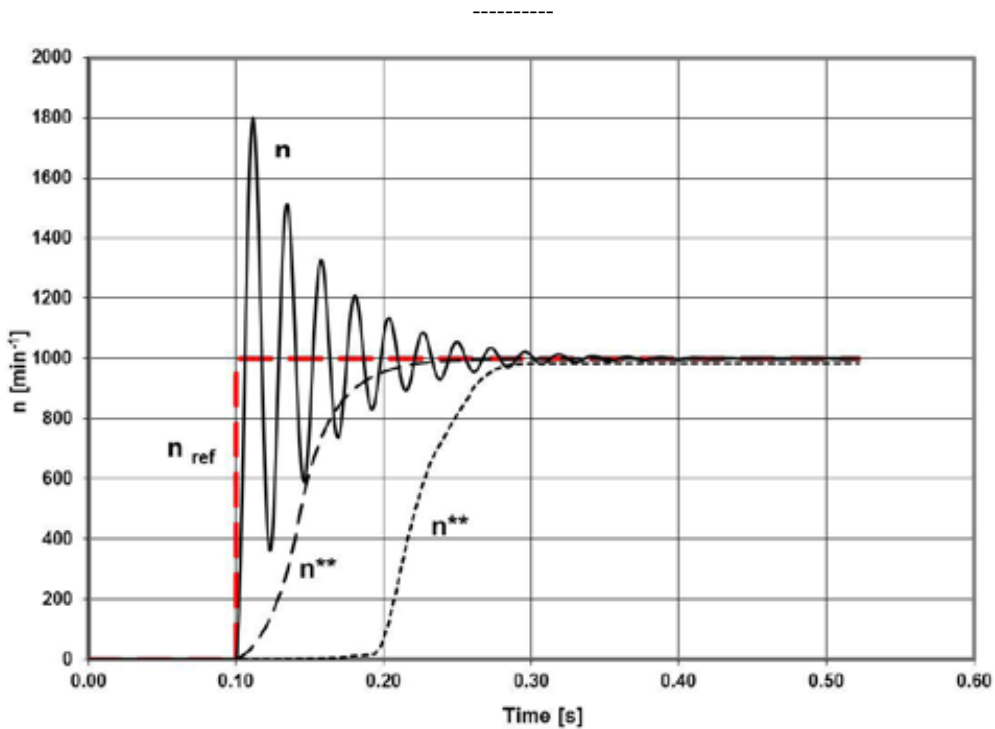


Figure 8: Comparison of all three models with step reference response.

For comparison, a step reference function was used (jump to the rotational speed of 1000 min^{-1}). In Figure 8 we can see that the responses are very different. In the simulation, the response marked n^* , is taken from the model, as detailed in [2]; n^{**} is taken from the source model [3]; n^{***} is a complete description of the electric model vector and frequency controller. In all three models, the same controller parameters were used and calculations were carried out by the same engine. In the first model, the actual situation (rotational speed is equal to the nominal) is not taken into account, while the default behaviour vector inverter is used as only proportional gain. The model response to n^{**} can be used for an asynchronous motor with very good dynamic properties. It comes down to the actual delay (dead zones), which the classic induction motor introduces, which is also revealed by experiment. Since only a P controller (controller gain parameter rotational speed set as recommended by the manufacturer) was used, there is also static error, which can be rectified by using the PI controller.

4 EXAMPLE OF PREASURE CONTROLL SIMULATION

A mathematical model of induction motor and frequency converter with the addition of model gear pump were chosen to for the purposes of comparing the results of the model. Furthermore, the results of tests on the experimental model described in [7] were added. Figure 9 shows the block diagram for the simulation package MATLAB-SIMULINK.

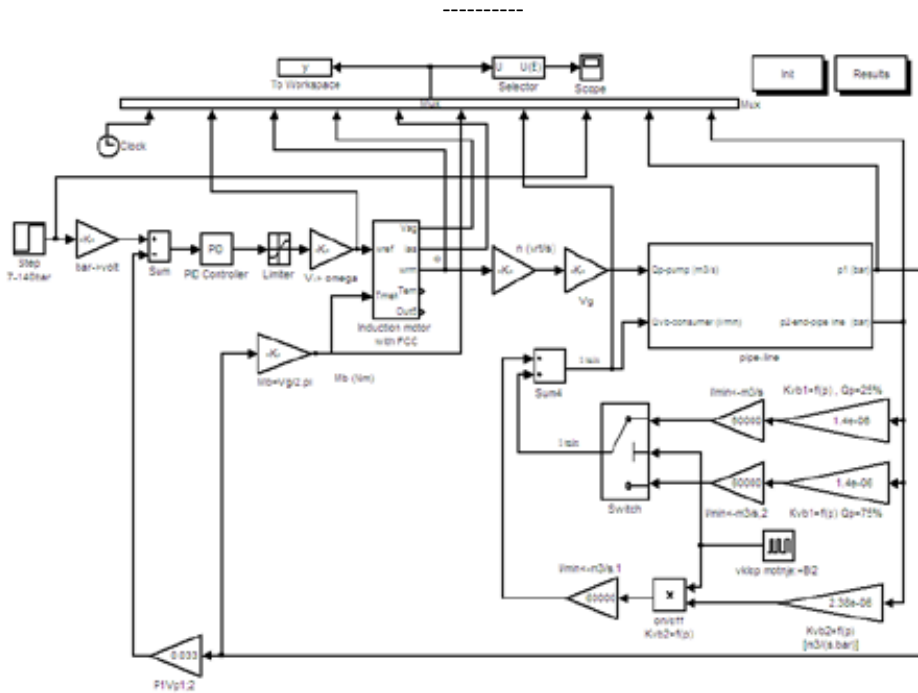


Figure 9: Block diagram for simulation of the pressure control

To simulate an actual environment, the experiments were conducted so that the pump was first employed to supply the hydraulic system with one consumer and then the next consumer was switched on/off by a directional control valve. Such experiments were repeated at different conditions, modelled by different lengths of pipe lines.

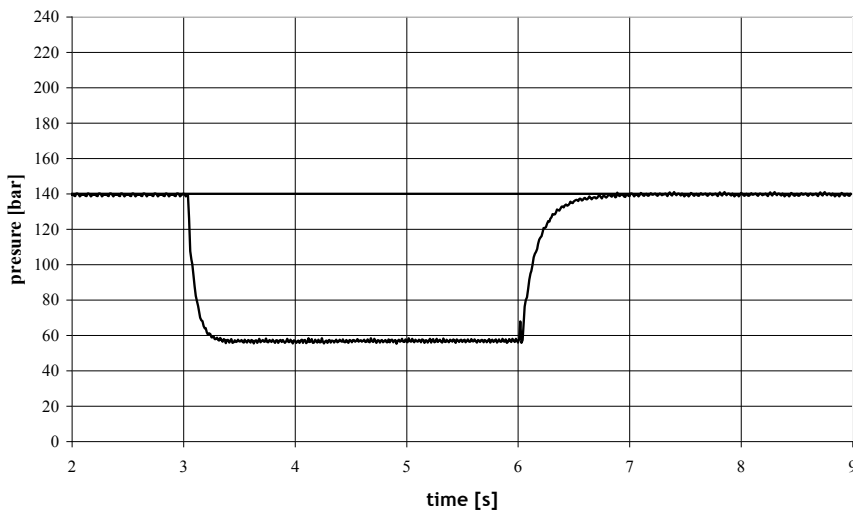


Figure 10: Pressure transient response at sudden switch –on/off of second consumer (open-loop response).

Tests of disturbance rejection were conducted at constant reference signal of 140 bars. The disturbance, i.e. the sudden switch-on of second consumer, produces a step change of pressure from 140 bar to 56 bar (see Fig. 10).

A comparison between simulated values and experimental values for the described test are presented in Figure 11.

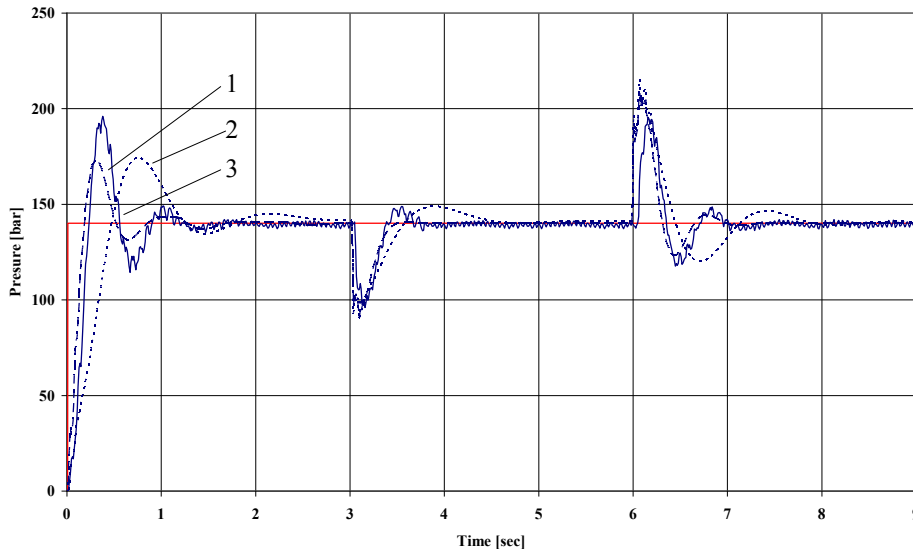


Figure 11: Comparison of simulated and experimental obtained values

(Dashed line 1- simulation detailed model, dotted line 2 – simulation conventional model, line 3 – experimental results)

5 CONCLUSIONS

The development of electronic components has also affected the implementation technique on the hydraulic power units.

Simulation of the behaviour of the whole system allows the correct selection of species and control components. The presented simulation model of induction motor and frequency controller provides an opportunity to take account of most of the phenomena ignored by the classic models (especially errors in the input network, errors in engine failure building the motor and its dynamic properties, etc.).

The model is intended for the less-experienced user (implemented as a block), while allowing complete control over the operation of the motor itself as the selected frequency controller.

The tests on experimental equipment show that usage of such simulation models covers real experiments. While the simulation model covers mostly a used combination of induction motor and frequency controller, results of new development of controllers must be added to the model. Therefore, fewer tests on experimental rigs are needed for establish the correct parameters for the selected dynamic behaviour of the whole system. The simulation also allows

simulation of errors on equipment (shut down of one power line, for example), which is normally very difficult to test on real equipment, due to possible damage of components or whole system.

References

- [1] P.C. Krause, O. Waszynek, S.D. Sudhoff: Analysis of Electric Machinery, IEE PRESS, 1995
- [2] I. Boldea, S.A. Nasar. Electric drives, IEE PRESS, CD, 1998
- [3] H.J. Bederke, R. Prassek, G. Rothenbach, P. Vaske, Elektrische Antriebe und Steuerung, B.G. Teubner, Stuttgart, 1975
- [4] D. Roseberg, Elektrische maschinen und antriebe, Munchen, Wien, Fachbuchverlag Leipzig in Carl-Hanser Verlag, 1999
- [5] R.H. Park, Two-Reaction Theory of Synchronous Machines-Generalized Method of Analysis-Part I, AIEE Trans., Vol. 48 July 1929, pp. 716–727
- [6] P.C. Krause, C.H. Thomas, Simulation of Symmetrical Induction Machine, IEEE Trans., Power Apparatuses and Systems, Vol. 84, November 1965, pp. 1038–1053
- [7] M. Kastrevc, Mathematical modeling of speed controlled hydraulic pumps, Ventil 8 (2002)3, pp. 162–167
- [8] M. Kastrevc, Dynamic Analysis of connection Induction motor and hydraulic gear pump, PhD. Thesis, Maribor, Slovenia, 2003

AUTHOR INSTRUCTIONS (MAIN TITLE)

SLOVENIAN TITLE

Authors, Corresponding author^{3†}

Key words: (Up to 10 keywords)

Abstract

Abstract should be up to 500 words long, with no pictures, photos, equations, tables, only text.

Povzetek

(In Slovenian language)

Submission of Manuscripts: All manuscripts must be submitted in English by e-mail to the editorial office at jet@uni-mb.si to ensure fast processing. Instructions for authors are also available online at www.fe.uni-mb.si/si/jet.html.

Preparation of manuscripts: Manuscripts must be typed in English in prescribed journal form (Word editor). A Word template is available at the Journal Home page.

A title page consists of the main title in the English and Slovenian languages; the author(s) name(s) as well as the address, affiliation, E-mail address, telephone and fax numbers of author(s). Corresponding author must be indicated.

Main title: should be centred and written with capital letters (ARIAL **bold** 18 pt), in first paragraph in English language, in second paragraph in Slovenian language.

Key words: A list of 3 up to 6 key words is essential for indexing purposes. (CALIBRI 10pt)

Abstract: Abstract should be up to 500 words long, with no pictures, photos, equations, tables, - text only.

Povzetek: - Abstract in Slovenian language.

^{3†} Corresponding author and other authors: Title, Name and Surname, Tel.: +XXX x xxx xxx, Fax: +XXX x xxx xxx, Mailing address: xxxxxxxxxxxxxxxxxxxxxxxxxxxxxxxxxxxx, E-mail address: email@xxx.xx

Main text should be structured logically in chapters, sections and sub-sections. Type of letters is Calibri, 10pt, full justified.

Units and abbreviations: Required are SI units. Abbreviations must be given in text when first mentioned.

Proofreading: The proof will be send by e-mail to the corresponding author, who is required to make their proof corrections on a print-out of the article in pdf format. The corresponding author is responsible to introduce corrections of data in the paper. The Editors are not responsible for damage or loss of manuscripts submitted. Contributors are advised to keep copies of their manuscript, illustrations and all other materials.

The statements, opinions and data contained in this publication are solely those of the individual authors and not of the publisher and the Editors. Neither the publisher nor the Editors can accept any legal responsibility for errors that could appear during the process.

Copyright: Submissions of a publication article implies transfer of the copyright from the author(s) to the publisher upon acceptance of the paper. Accepted papers become the permanent property of “Journal of Energy Technology”. All articles published in this journal are protected by copyright, which covers the exclusive rights to reproduce and distribute the article as well as all translation rights. No material can be published without written permission of the publisher.

Chapter examples:

1 MAIN CHAPTER

(Arial bold, 12pt, after paragraph 6pt space)

1.1 Section

(Arial bold, 11pt, after paragraph 6pt space)

1.1.1 Sub-section

(Arial bold, 10pt, after paragraph 6pt space)

Example of Equation (lined 2 cm from left margin, equation number in normal brackets (section.equation number), lined right margin, paragraph space 6pt before in after line):

$$c = \sqrt{a^2 + b^2} \tag{1.1}$$

Tables should have a legend that includes the title of the table at the top of the table. Each table should be cited in the text.

Table legend example:

Table 1: Name of the table (centred, on top of the table)

Figures and images should be labelled sequentially numbered (Arabic numbers) and cited in the text – Fig.1 or Figure 1. The legend should be below the image, picture, photo or drawing.

Figure legend example:

Figure 1: Name of the figure (centred, on bottom of image, photo, or drawing)

References

[1] Name. Surname: Title, Publisher, p.p., Year of Publication

Example of reference-1 citation: In text, Predin, [1], text continue. **(Reference number order!)**

SiPRO
INŽENIRING

Gen
ENERGIJA

JET

JET

Journal of ENERGY TECHNOLOGY

Vol. 5/3 2012

UNIVERSITY OF MARIBOR, FACULTY OF ENERGY TECHNOLOGY



9 771855 574008

ISSN 1855-5748